The large-scale freshwater cycle of the Arctic — **Source link** ↗

Mark C. Serreze, Andrew P. Barrett, Andrew G. Slater, Rebecca A. Woodgate ...+6 more authors

Institutions: Cooperative Institute for Research in Environmental Sciences, University of Washington, University of New Hampshire, British Antarctic Survey

Topics: Arctic dipole anomaly, Arctic sea ice decline, Arctic geoengineering, Arctic ice pack and Arctic

Related papers:

- The role of sea ice and other fresh water in the Arctic circulation

- Increasing river discharge to the Arctic Ocean

- Beaufort Gyre freshwater reservoir: State and variability from observations

- Current estimates of freshwater flux through Arctic and subarctic seas

- Revising the Bering Strait freshwater flux into the Arctic Ocean

11-21-2006

The large-scale freshwater cycle of the Arctic

Mark C. Serreze
University of Colorado, Boulder

Andrew P. Barrett
University of Colorado, Boulder

Andrew G. Slater
University of Colorado, Boulder

Rebecca A. Woodgate
University of Washington

Knut Aagaard
University of Washington

See next page for additional authors

Recommended Citation

Serreze, M.C., A.P. Barrett, A.G. Slater, R.A. Woodgate, K. Aagaard, R.B. Lammers, M. Steele, R. Moritz, M. Meredith, and C.M. Lee (2006), The large-scale freshwater cycle of the Arctic, J. Geophys. Res., 111, C11010, doi: 10.1029/2005JC003424.

Authors

Mark C. Serreze, Andrew P. Barrett, Andrew G. Slater, Rebecca A. Woodgate, Knut Aagaard, Richard B. Lammers, Michael Steele, Richard Moritz, Michael Meredith, and Craig M. Lee

The large-scale freshwater cycle of the Arctic

Mark C. Serreze,[1] Andrew P. Barrett,[1] Andrew G. Slater,[1] Rebecca A. Woodgate,[2]
Knut Aagaard,[2] Richard B. Lammers,[3] Michael Steele,[2] Richard Moritz,[2]
Michael Meredith,[4] and Craig M. Lee[5]

[1] This paper synthesizes our understanding of the Arctic's large-scale freshwater cycle. It combines terrestrial and oceanic observations with insights gained from the ERA-40 reanalysis and land surface and ice-ocean models. Annual mean freshwater input to the Arctic Ocean is dominated by river discharge (38%), inflow through Bering Strait (30%), and net precipitation (24%). Total freshwater export from the Arctic Ocean to the North Atlantic is dominated by transports through the Canadian Arctic Archipelago (35%) and via Fram Strait as liquid (26%) and sea ice (25%). All terms are computed relative to a reference salinity of 34.8. Compared to earlier estimates, our budget features larger import of freshwater through Bering Strait and larger liquid phase export through Fram Strait. While there is no reason to expect a steady state, error analysis indicates that the difference between annual mean oceanic inflows and outflows ($\sim$8% of the total inflow) is indistinguishable from zero. Freshwater in the Arctic Ocean has a mean residence time of about a decade. This is understood in that annual freshwater input, while large ($\sim$8500 km^3), is an order of magnitude smaller than oceanic freshwater storage of $\sim$84,000 km^3. Freshwater in the atmosphere, as water vapor, has a residence time of about a week. Seasonality in Arctic Ocean freshwater storage is nevertheless highly uncertain, reflecting both sparse hydrographic data and insufficient information on sea ice volume. Uncertainties mask seasonal storage changes forced by freshwater fluxes. Of flux terms with sufficient data for analysis, Fram Strait ice outflow shows the largest interannual variability.

Citation: Serreze, M. C., A. P. Barrett, A. G. Slater, R. A. Woodgate, K. Aagaard, R. B. Lammers, M. Steele, R. Moritz, M. Meredith, and C. M. Lee (2006), The large-scale freshwater cycle of the Arctic, *J. Geophys. Res.*, *111*, C11010, doi:10.1029/2005JC003424.

1. Introduction

[2] The Arctic freshwater system is shaped by a remarkable conjunction of latitude, geography, and marine processes, and its climatic impacts extend beyond the Arctic. In this paper we provide a modern view of this system, synthesizing information gathered over the past decade to document the principal pathways between the atmospheric, terrestrial, and oceanic components. We consider oceanic freshwater storage, as well as seasonal and interannual variability, and we provide an updated and expanded view of the Arctic Ocean's annual mean freshwater budget. Early constructions of that budget (or its salt equivalent) struggled

with serious data deficiencies [e.g., *Mosby*, 1962; *Aagaard and Greisman*, 1975], and it was not until *Östlund and Hut* [1984] introduced oxygen isotope methodology that the relative roles of ice and liquid freshwater in the overall balance became visible. Our approach and perspective here substantially follow the seminal work of *Aagaard and Carmack* [1989] and the subsequent paper by *Carmack* [2000]. Our study also complements, and draws from, that of *Dickson et al.* [2006], which focuses on ocean flux terms.

[3] As in the study by *Aagaard and Carmack* [1989], oceanic freshwater fluxes and storages are computed relative to a salinity of 34.8 on the dimensionless practical salinity scale (PSS-78). Details are provided in section 2.3. Data are drawn from coordinated national and international efforts such as the Arctic System Science (ARCSS) Freshwater Initiative (FWI) of the National Science Foundation; Variability of Exchanges in the Northern Seas (VEINS, http://www.ices.dk/ocean/project/veins); Arctic and Subarctic Ocean Fluxes (ASOF, http://asof.npolar.no); and the Arctic Ocean Model Intercomparison Project (AOMIP, http://fish.cims.nyu.edu/project_aomip/overview.html). These efforts have provided new estimates of ocean transports from observations, remote sensing and coupled models. FWI efforts are also capitalizing on data from

[1]Cooperative Institute for Research in Environmental Sciences, University of Colorado, Boulder, Colorado, USA.
[2]Polar Science Center, Applied Physics Laboratory, University of Washington, Seattle, Washington, USA.
[3]Water Systems Analysis Group, University of New Hampshire, Durham, New Hampshire, USA.
[4]British Antarctic Survey, Cambridge, UK.
[5]Ocean Physics Department and Applied Physics Laboratory, University of Washington, Seattle, Washington, USA.
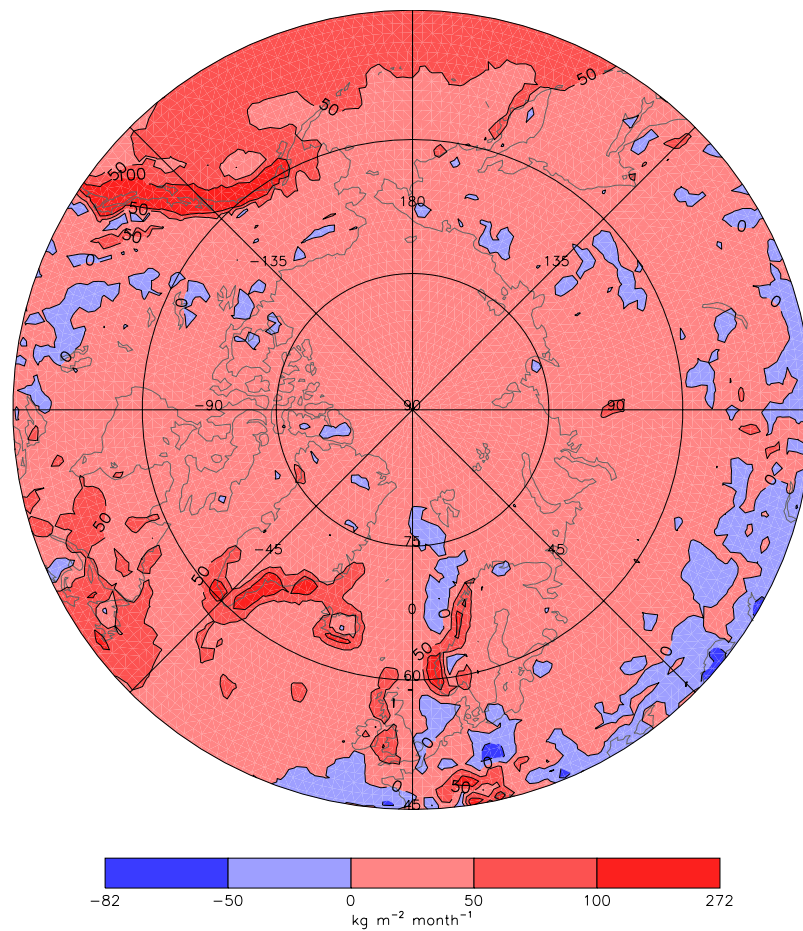
Figure 1. Annual mean (1979–2001) field of the vapor flux convergence (equivalent to P-ET) over northern high latitudes in simplified form. Calculations use vertical integrals of the vapor flux divergence from the European Centre for Medium-Range Weather Forecasts (ECMWF) ERA-40 reanalysis.

atmospheric reanalysis, field programs, river gauging networks, and hydrologic and land surface models that quantify the atmospheric and terrestrial branches of the system. The Arctic Regional Integrated Monitoring System (RIMS, http://rims.unh.edu), a component of the FWI, harmonizes such data sources for monitoring and historical analysis of the terrestrial freshwater cycle.

[4] We begin by qualitatively describing the main features of the system, starting with the delivery of freshwater to the Arctic Ocean from the surrounding landmasses of North American and Eurasia.

[5] In the long-term annual mean (here computed for 1979–2001), the land region north of 50°N is primarily an area of vapor flux convergence (Figure 1), so that precipitation (P) exceeds evapotranspiration (ET). The net precipitation (P-ET) represents water available for runoff. A large part of this land area drains northward, and over some 15.8×10^6 km^2 four of the world's major river systems (the Ob, Yenisey, and Lena in Eurasia, and the Mackenzie in Canada) empty into the comparatively small (9.6×10^6 km^2) and largely enclosed Arctic Ocean. Figure 2 shows the bounds of the Arctic Ocean and its contributing terrestrial drainage; domains are defined below.

[6] The Arctic Ocean is also freshened from two other major sources. One is net precipitation over the Arctic Ocean itself, while the other is import of low-salinity water (relative to the Arctic Ocean reference of 34.8) through the narrow Bering Strait (Figure 2). This mean northward flow is driven by the pressure gradient between the Pacific and Arctic oceans [*Shtokman*, 1957; *Gudkovich*, 1962; *Coachman and Aagaard*, 1966; *Stigebrandt*, 1984], established at least in part by salinity and temperature differences between the basins. Flow variability is large [*Woodgate et al.*, 2005a] and correlated with the local wind [e.g., *Coachman and Aagaard*, 1981; *Aagaard et al.*, 1985], which in the mean opposes the oceanic pressure gradient [*Woodgate et al.*, 2005b].

[7] The largest freshwater sinks are southward flows into the Atlantic. These are via (1) the complex channels of the Canadian Arctic Archipelago, and (2) Fram Strait, between northern Greenland and Svalbard (Figure 2). There is also a small southward flux through the western Barents Sea that we ignore in this study. The flux through the Canadian Arctic Archipelago is primarily in liquid form [*Steele et al.*, 1996; *Prinsenberg and Hamilton*, 2005]. In contrast, the Fram Strait freshwater sink includes a large sea ice flux, as well as that of low-salinity liquid water in the upper ocean [*Östlund and Hut*, 1984; *Aagaard and Carmack*, 1989; *Dickson et al.*, 2006]. The formation and growth of sea ice distills water, and as ice forms, brine is rejected into the
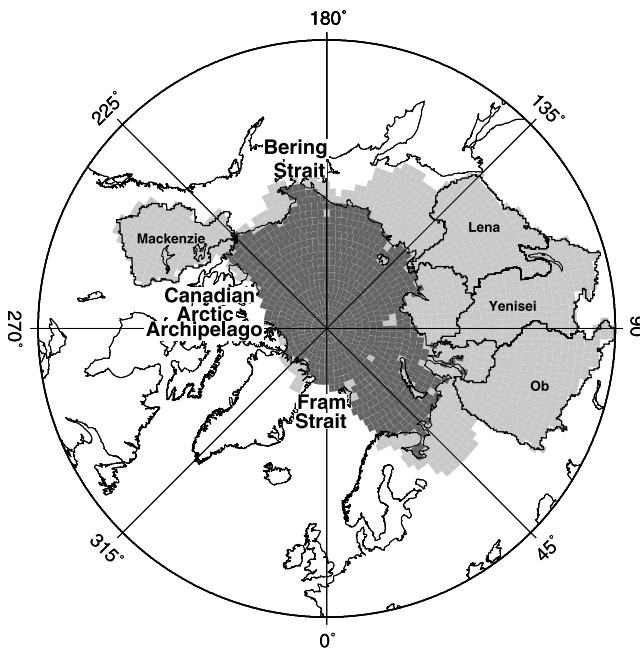
Figure 2. Location map showing the Arctic Ocean domain as defined for the present study (dark shading) and the land regions that drain into it (light shading). See text for further discussion. Key geographic features are listed, including boundaries of the four largest Arctic-draining watersheds: the Ob, Yenisei, Lena, and Mackenzie.

underlying ocean. Even during the spring warming, when ice is no longer growing, brine cells are draining. Sea ice has typical salinities of only 2–6 (PSS-78). As a result, although the Arctic sea ice cover is typically only about 1–4 m in thickness, the ice flux through Fram Strait is an efficient mechanism for exporting freshwater. There is also deeper outflow through Fram Strait, with salinity higher (>34.9 [*Aagaard et al.*, 1991; *Dickson et al.*, 2006]) than the Arctic Ocean reference of 34.8. Consequently, this deeper transport counts as a freshwater source.

[8] Another sink is the poleward flow of Atlantic-derived waters into the Arctic Ocean. This occurs in two main branches, one in eastern Fram Strait and the other in the Barents Sea (referred to respectively as the Fram Strait and Barents Sea branches [*Rudels et al.*, 1994]). These northward flows are freshwater sinks because of their initially high salinity (35.0–35.2) [*Aagaard and Carmack*, 1989]. Recent studies suggest that the Barents Sea Branch is partly freshened by sea ice exiting the Arctic Ocean into the Barents Sea [*Aagaard and Woodgate*, 2001; *Woodgate et al.*, 2001; *Kwok et al.*, 2005].

[9] Prominent annual cycles characterize several components of the Arctic freshwater cycle. For most of the year, net precipitation over land is stored as snow. River discharge to the Arctic Ocean therefore has a strong spring maximum due to snowmelt, with 60% occurring from April through July [*Lammers et al.*, 2001]. Net precipitation over the Arctic Ocean tends to peak in late summer and early autumn [*Walsh et al.*, 1994], reflecting seasonality in the atmospheric circulation and large open water areas that provide a moisture source. Also reflecting changes in the

atmospheric circulation, the Fram Strait ice flux generally peaks in winter, with a summer minimum [*Vinje*, 2001]. This contrasts with the Bering Strait inflow and the Canadian Arctic Archipelago outflow, which are largest in summer [*Woodgate and Aagaard*, 2005; *Prinsenberg and Hamilton*, 2005]. The West Spitsbergen Current has a northward maximum in winter [*Hanzlick*, 1983; *Fahrbach et al.*, 2001], although it is uncertain how much of the flow recirculates in Fram Strait. Indeed, *Jonsson* [1989] suggested that the inflow to the Arctic Ocean does not show a significant seasonal cycle. On the basis of a recent assessment of moored and hydrographic measurements during 1997–2001, the Barents Sea Branch tends to be larger in winter than in summer but is highly variable [*Ingvaldsen et al.*, 2004].

[10] Interannual variability in some of the budget terms is apparent, in particular the Fram Strait ice outflow [e.g., *Vinje et al.*, 1998; *Vinje*, 2001], and it is not clear how long a record is required to obtain a stable mean value. Additionally, several terms show trends. For example, discharge from Siberian rivers has shown a modest general upward trend since the mid-1930s [*Peterson et al.*, 2002], while *Rothrock et al.* [1999] and *Cavalieri et al.* [2003] respectively document downward trends in sea ice thickness and extent over the past several decades.

[11] Why should the Arctic freshwater cycle concern us? In the cold Arctic Ocean, the density stratification is predominantly determined by salinity, not temperature. Freshwater from runoff, P-ET, and the Bering Strait inflow help keep the upper 200 m of the water column relatively fresh. The resulting strong density stratification inhibits vertical mixing with warmer, saline Atlantic waters below ~200 m, allowing sea ice to form [*Aagaard and Coachman*, 1975]. Through latent heat release, that ice formation represents a significant heat source to the atmosphere. As the ice thickens, it then increasingly decouples the cold atmosphere from the ocean. During summer, on the other hand, the Arctic is kept cool through the high ice albedo and by heat loss to ice melt. Ice growth and melt thus have pronounced impacts on the Arctic heat budget and consequently impose requirements for poleward atmospheric energy transport [*Nakamura and Oort*, 1988].

[12] Oceanic freshwater transfers across the Arctic reduce the salinity contrast between the Atlantic and Pacific, and thus link large parts of the global ocean system. The freshwater outflow from the Arctic Ocean may also interact with the large-scale meridional overturning circulation (MOC). Numerous studies [e.g., *Wehl*, 1968; *Aagaard and Carmack*, 1989; *Steele et al.*, 1996; *Häkkinen*, 1999; *Holland et al.*, 2001; *Proshutinsky et al.*, 2002; *Dukhovskoy et al.*, 2004; *Curry and Mauritzen*, 2005] suggest that the MOC could be disrupted by increases in freshwater outflow from the Arctic to the Atlantic Ocean that increase upper ocean stratification in the convective regions. The Arctic Ocean itself contains a very large store of freshwater: relative to salinity 34.8, the liquid storage is about 74,000 km³ in the annual mean, with another 10,000 km³ as sea ice (see section 4). During the North Atlantic "Great Salinity Anomaly" (GSA) of the late 1960s and early 1970s, a strong pulse of sea ice outflow through Fram Strait appears to have stopped convection in the Labrador Sea for a year [*Dickson et al.*, 1988; *Aagaard and Carmack*, 1989].
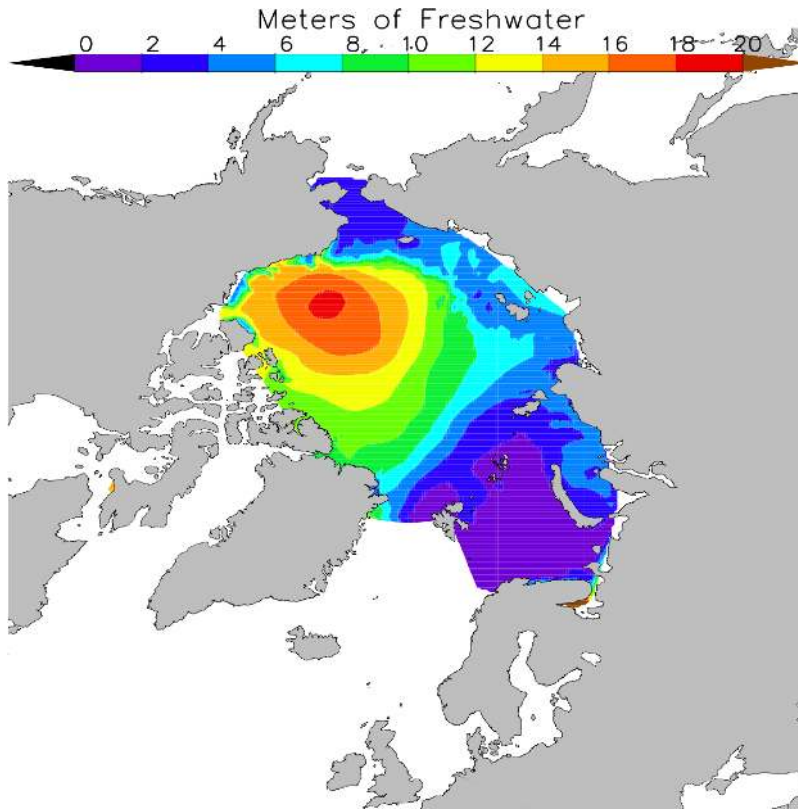
Figure 3. Mean annual freshwater content of the Arctic Ocean (excluding sea ice) based on the University of Washington Polar Science Center Hydrographic Climatology (PHC). The scale is in meters of freshwater, computed using a reference salinity of 34.8 (http://psc.apl.washington.edu/Climatology.html).

[13] In response to the mean Beaufort Sea atmospheric anticyclone that promotes Ekman convergence, much of the liquid portion of the Arctic Ocean's freshwater is stored in the Beaufort Gyre (Figure 3). *Proshutinsky et al.* [2002] suggest that release of only a few percent of this freshwater could cause a North Atlantic salinity anomaly comparable to the GSA. *Dukhovskoy et al.* [2004] extend some of these ideas, and suggest an auto-oscillatory mechanism for decadal variability in the Arctic's coupled ocean/atmosphere system, involving freshwater and heat exchanges between the Arctic Ocean and the Nordic seas.

[14] Our objective is to assess the Arctic freshwater budget with modern data, and to document the primary pathways between the atmospheric, terrestrial, and oceanic components. Section 2 formalizes the budget framework and discusses the ocean and terrestrial domains (Figure 2). Primary data sets are introduced in section 3. Section 4 discusses annual means of individual terms and constructs a schematic of the annual mean freshwater cycle. Seasonal and interannual variability are addressed in section 5.

2. Budget Framework

2.1. Formal View

[15] Consider an atmospheric column, extending from the surface to the top of atmosphere. The freshwater budget of such a column can be expressed as

$$\partial W/\partial t = ET - P - \nabla \bullet \mathbf{Q} \tag{1}$$

where $\partial W/\partial t$ represents the change in precipitable water (W) in the atmosphere (the water depth of the vapor in the column), ET is the surface evapotranspiration rate, P is the precipitation rate and $\nabla \bullet \mathbf{Q}$ is the divergence of the horizontal water vapor flux $\mathbf{Q}$ integrated from the surface to the top of the column. Thus ET increases precipitable water, precipitation decreases precipitable water and horizontal divergence of the water vapor flux decreases precipitable water. For long-term annual means and assuming a steady state, the first term of equation (1) can be dropped, meaning that net precipitation (P-ET) equals the negative of the vapor flux divergence (i.e., the convergence). Although ET equals E over the ocean, for simplicity we use the term ET for both land and ocean. Equation (1) ignores the small effects of phase transformations in the atmosphere represented by clouds, as well as convergence of water in liquid and solid phases.

[16] Oceanic and terrestrial columns can be similarly studied. Consider columns extending from the surface to a depth at which freshwater transports are negligible. For the land column:

$$\partial M/\partial t = P - ET - R \tag{2}$$

where M is the water content of the column and R represents the combination of surface and subsurface runoff, which eventually finds its way out of the domain. For the oceanic column, a slightly different expression applies:

$$\partial M/\partial t = P - ET + R - \nabla \bullet \mathbf{F} \tag{3}$$
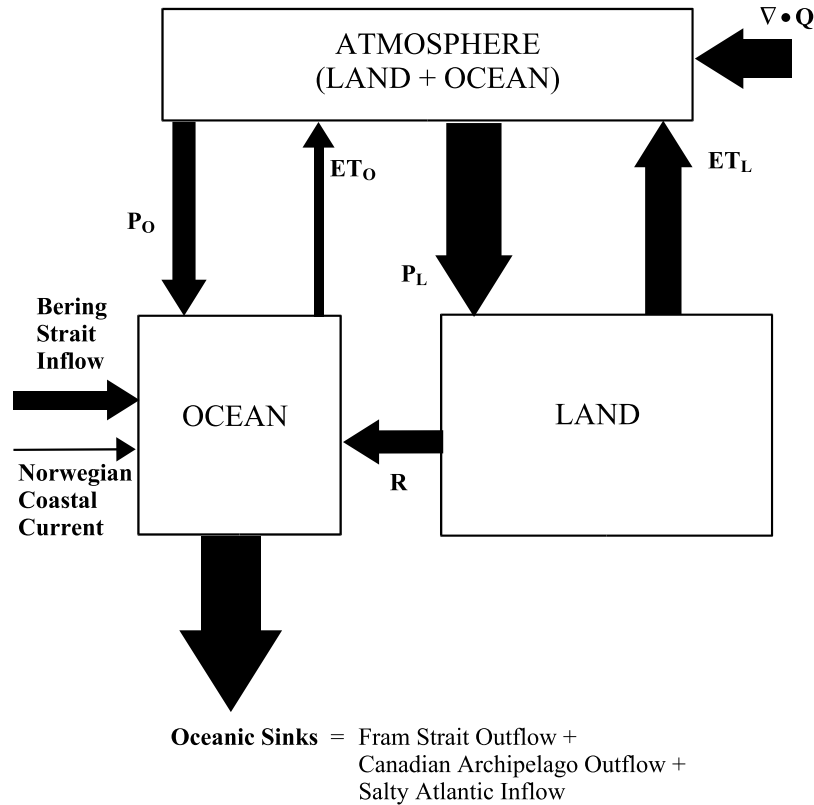
Arctic Basin Freshwater Budget Schematic

Figure 4. Schematic of the Arctic's large-scale freshwater cycle. The atmospheric box combines the land and ocean domains. The boxes for land and ocean are sized proportional to their areas. R is runoff, P is precipitation, ET is evapotranspiration, and Q is the vapor flux. Subscript "L" and "O" denote land and ocean, respectively.

where $\partial M/\partial t$ is the depth-integrated (1000 m) change in freshwater content and $\nabla \bullet F$ is the depth-integrated horizontal divergence of the oceanic freshwater flux in liquid and solid phase. Again, for long-term annual means, and assuming steady state, the time derivative terms can be dropped.

[17] Figure 4 links together the primary components of the annual mean budget in simple schematic form, grouping the various net oceanic freshwater sinks. The principal ocean flux terms are the Bering Strait inflow, outflow through Fram Strait and the channels of the Canadian Archipelago and Atlantic water inflow (the Fram Strait and Barents Sea branches). There is also a relatively small freshwater transport into the Arctic Ocean via the Norwegian Coastal Current which enters through the Barents Sea. It essentially represents the inflow of Baltic and North Seawaters, together with runoff from the Scandinavian coast. The width of the arrows in Figure 4 indicates the relative magnitudes of the fluxes. We will expand upon and quantify this schematic in section 4.

[18] Our framework ignores a number of other small oceanic terms [see *Aagaard and Carmack*, 1989]. Runoff estimates include contributions from the Greenland Ice Sheet only through extrapolation of observed runoff to the

ungauged area of the land surface (see section 3.3). The annual delivery of ice from the north shore of Greenland to the Arctic Ocean via the larger glaciers has been estimated at 7.9 km³ [*Rignot et al.*, 2001; M. Fahnestock, personal communication, 2005]. This is very small relative to other fluxes considered in this paper (see section 4.1).

2.2. Terrestrial and Ocean Domains

[19] The boundaries of the Arctic Ocean (Figure 2) were primarily determined by drawing lines across several straits. The natural boundary between the Arctic and Pacific oceans is the Bering Strait. Natural boundaries between the Arctic Ocean and Atlantic are Fram Strait and the passage between Svalbard and northern Scandinavia. The other Atlantic connection is through the straits of the Canadian Arctic Archipelago. We adopt a boundary extending across the northern end of the archipelago. A digital river network was then used to define the land areas draining into the ocean domain. The ocean and land domains have areas of 9.6×10^6 km² and 15.8×10^6 km² respectively. The ocean domain approximates that used by *Aagaard and Carmack* [1989]. A different ocean definition would yield a different terrestrial domain. For example, *Serreze et al.* [2002] viewed the Arctic Ocean as including Hudson and James

Bay, Baffin Bay, and part of the northern North Atlantic. Their contributing terrestrial drainage was consequently much larger.

2.3. Units and Reference Salinity

[20] Freshwater fluxes are provided in units of km^3 and mm per unit time (month or year). The latter represents water depth averaged over each domain and from hereon is referred to as yield. Stores are given in km^3 and mm. For fluxes, some readers are more familiar with the Sverdrup (Sv) unit. The conversion is 1 Sv = 10^6 m^3 s^{-1} = 31,536 km^3 per year.

[21] Mention has already been made of reference salinity. Consistent with most previous literature, including *Aagaard and Carmack* [1989] an Arctic Ocean reference of 34.8 is adopted. Total water fluxes are converted to freshwater fluxes as follows:

$$F_{FW} = F_T(1 - SAL/REF) \qquad (4)$$

Where F_{FW} is the freshwater flux, F_T is the total water flux, SAL is the bulk salinity of the total flux, and REF is the reference salinity. Simply put, if the bulk salinity of the total flux is less than (greater than) the adopted reference, the flux represents a freshwater source (sink) to the Arctic Ocean. The same general approach can be used to obtain oceanic freshwater stores through vertical integration of archived salinity data. These freshwater storage estimates ignore "negative freshwater", i.e., waters saltier than the 34.8 reference.

[22] While reference salinity is arbitrary, the value of 34.8 is pragmatic in being a reasonable estimate of the average salinity of the Arctic Ocean. The 34.8 salinity surface lies roughly at the 200–300 m level, above which most of the ocean freshwater resides [*Aagaard and Carmack*, 1989]. The sign of a freshwater flux hence represents the tendency effect of that flux component on the mean salinity of the Arctic Ocean. Some studies [e.g., *Dickson et al.*, 2006] have preferred to use an Arctic Ocean reference of 35.2, which represents the maximum salinity of Atlantic-derived waters. Using this higher value, the volume and freshwater transports will all be in the same direction for all individual streams. Building on earlier discussion, using the reference of 34.8 means that the Atlantic inflow to the Arctic Ocean, with a bulk salinity of ~35.0, is a sink since it acts to increase the salinity of the Arctic Ocean. By contrast, it would be a freshwater source using the higher 35.2 reference. Similarly, the deeper component of the southward Fram Strait water flux, with a bulk salinity of 34.9, is a freshwater source with the lower reference but a sink with the higher reference.

3. Primary Data Sets

3.1. ERA-40 Reanalysis and Observed Precipitation

[23] Our atmospheric terms are based mainly on data from the European Centre for Medium Range Forecasts (ECMWF) ERA-40 reanalysis. Reanalysis is a retrospective form of numerical weather prediction (NWP), whereby long time series of gridded atmospheric fields and surface state variables and fluxes are obtained by assimilating observations (primarily free-air variables such a tropospheric winds,

humidity and pressure heights) within a global coupled atmospheric/land surface modeling framework. Sea ice cover, sea surface temperature and land surface vegetation are prescribed from observations. Unlike NWP systems used for operational weather forecasting that are undergoing continual refinement, reanalyses use fixed versions of the atmospheric model/data assimilation system. This yields more temporally consistent fields. Inconsistencies may still be present due to changes in the assimilation database through time.

[24] We use ERA-40 data for the period 1979–2001. ERA-40 provides estimates of P, ET, P-ET and precipitable water. For land, ERA-40 also computes estimates of snow water equivalent. Vertical integrals of moisture terms are part of the ERA-40 archive. Precipitation is calculated as 6-hour accumulations from 6-hour forecasts. ET is based on averages over each 6-hour forecast. ERA-40 fields are available back to 1957, but those from 1979 incorporate data from the modern satellite record and are more reliable. Figure 1 is based on the annual mean vapor flux convergence (P-ET, see equation (1)) from ERA-40.

[25] Six-hourly fields are available from the National Center for Atmospheric Research (NCAR) on a grid with an approximate 125 km spacing (the N80 grid). Overviews of ERA-40 can be found at the ECMWF Web site (www.ecmwf.int/research/era/Products). Data sources rely strongly on archives used in the companion National Centers for Environmental Prediction/NCAR (NCEP/ NCAR) reanalysis. ERA-40 makes heavy use of multichannel satellite radiances. Compared to the precursor ECMWF ERA-15 (1979–1993) effort there are numerous improvements in the land surface scheme and sea ice boundary fields.

[26] ERA-40 precipitation estimates over the Arctic (both land and ocean) are known to be greatly improved over those from NCEP/NCAR, although the model has generally less precipitation than observations [*Serreze et al.*, 2005; *Betts et al.*, 2003]. The validation study of *Serreze et al.* [2005] employed a gridded monthly data set (1979–1993) of observed precipitation for the region north of 45°N (excluding open ocean regions). These fields blend data from several sources (including Arctic Ocean data from the Russian "North Pole" drifting camps through 1991), adjusted for gauge undercatch of solid precipitation and other problems using the climatological bias adjustments of *Legates and Willmott* [1990]. Our study complements ERA-40 precipitation with values from the *Serreze et al.* [2005] data set.

[27] The term P-ET can be calculated from reanalysis data in two ways. Following equation (1), there is the aerological method, whereby long-term annual means of P-ET equate to the vertically integrated vapor flux divergence. The other method is to calculate P-ET from the forecasts of P and ET.

[28] Several earlier studies have examined P-ET for the region north of 70°N, the "polar cap", using data from NCEP/NCAR and ERA-15. Aerological estimates from ERA-40 for the polar cap compare favorably. Long-term annual means from ERA-15 and NCEP/NCAR range from 182 to 207 mm [*Genthon*, 1998; *Cullather et al.*, 2000], compared 193 mm from ERA-40 (calculated from 1979 to 2001) Aerolological estimates from reanalysis are higher than those based solely on analysis of rawinsonde data

(atmospheric soundings), either through simple interpolation of meridional vapor fluxes to 70°N [*Serreze et al.*, 1995; *Walsh et al.*, 1994] or using more robust methods [*Gober et al.*, 2003]. This is not surprising. As shown by *Cullather et al.* [2000], the high-latitude rawinsonde network is insufficient to capture the moisture "pathways" into the polar cap. Aerological estimates from reanalysis, based on a blend of observations and a short-term forecast, capture these pathways.

[29] Another conclusion is that P-ET from reanalysis based on the aerological method and from the forecasts of P and ET are not in balance, with lower P-ET in the forecasts. If the model did not assimilate observations, conservation of mass would dictate balance. The imbalance results primarily from nudging the model humidity toward observations. *Cullather et al.* [2000] (1979–1993) cite an imbalance over the polar cap of 50 mm for ERA-15, compared to 82 mm for NCEP/NCAR. For ERA-40, we calculate a smaller imbalance of 15 mm.

3.2. CHASM Land Surface Model

[30] Part of the ERA-40 system is its land surface model (LSM), which is coupled to the atmospheric model. To complement output from ERA-40, we examine the impacts of varying land surface treatments on modeled ET and runoff. To this end, we use output from two versions of the Chameleon Surface Model (CHASM) [*Desborough*, 1999], driven with ERA-40 inputs (1979–2001) interpolated to a network of 1576 100 × 100 km grid cells covering the terrestrial domain (Figure 2). The ERA-40 drivers for these simulations include incoming solar and longwave radiation, low-level winds, humidity and precipitation at 3-hour time steps.

[31] CHASM can be run in several modes, although only the two most complex cases are applied here. Under these, vegetation modeling follows *Deardorff* [1978], in which there is an explicit foliage layer. There is a root zone soil moisture reservoir that operates similar to the *Manabe* [1969] bucket formulation but reservoir capacities are not globally constant. The soil thermal regime is computed using a five-layer diffusion model that accounts for phase change. The snowpack is modeled as a composite layer, where the topsoil layer and snowpack share the same temperature [*Slater et al.*, 2001]. Snow albedo is computed as a time-based exponential decay function. Fractional snow cover is a function of surface roughness length. Vegetation and soil parameters follow those used in Phase 2 of the Global Soil Wetness Project [*Dirmeyer et al.*, 1999].

[32] The first simulation is a single tile case (termed CHASM1), where each grid box operates as one entity with a single surface energy balance, employing mean "effective" parameters that represent the net effects of the bare ground and vegetation in the box. The second is a dual tile case (termed CHASM2) where separate surface energy balances are computed for the bare ground and vegetated portions of the grid box.

3.3. River Discharge and Runoff

[33] Gauge records of monthly river discharge were obtained from R-ArcticNET [*Lammers et al.*, 2001; *Shiklomanov et al.*, 2002]. We use records from gauges closest to the mouths of rivers draining into the Arctic

Ocean for the period 1980–1999. Data availability from Canada and Russia precludes assembling records for more recent years. The number of gauges with records in any given month ranges from 17 to 43 representing the monitoring of 61% to 81% of the total drainage area. Aggregated gauged discharge was converted into runoff (yield). It was assumed that runoff from the ungauged area is identical to that for the gauged area. Multiplication by area yields discharge for the ungauged area. We feel this method will introduce only small errors in the monthly climatologies and annual time series.

3.4. Oceanic Freshwater Fluxes

[34] Several studies [*Vinje et al.*, 1998; *Vinje*, 2001; *Widell et al.*, 2003; *Kwok et al.*, 2004] provide recent estimates of the Fram Strait sea ice volume export, which we adjusted to freshwater transports with a salinity of 4 and an ice density of 900 kg m^{-3}. The volume transports from *Vinje et al.* [1998] are from August 1990 through July 1996. They combine information on ice thickness across the strait using upward looking sonar (ULS), ice velocity from drifting buoys, the difference in sea level pressure (SLP) between Fram Strait and the central core of the northern North Atlantic trough (the mean trough of low atmosphere pressure extending into Arctic latitudes), and the width of the ice stream. The pressure difference is a proxy for the geostrophic wind. *Vinje* [2001] used a similar approach to provide a longer record from 1950 to 2000. *Kwok et al.* [2004] provide volume transports from October 1991 through September 1999. They use ice thickness from ULS combined with an area flux, based on a feature tracking method applied to data from the Special Sensor Microwave/Imager (SSM/I). Because of contamination of the microwave scattering signal by melt effects, this approach cannot provide area fluxes for the period June–September. For these months, estimates (summed over the four month periods of each year) rely on regression between time series of ice area flux and the SLP gradient across the strait. The estimates from *Widell et al.* [2003] are based on data from moored Doppler current meters over the period 1996–2000.

[35] Recent observations quantify the total Fram Strait liquid volume transport [*Fahrbach et al.*, 2001; *Schauer et al.*, 2004], but there are few estimates of the liquid freshwater flux. *Meredith et al.* [2001] used velocity data from moorings and sections of salinity and oxygen isotopes (August–September 1997 and 1998) that enable separation of ice melt and meteoric water, associated with the combined influences of P-ET over the ocean and river discharge. *Dickson et al.* [2006] provide an updated observationally based estimate of the deeper ocean transport through Fram Strait relative to a salinity of 35.2, which we adjusted to 34.8.

[36] *Woodgate and Aagaard* [2005] have assembled improved estimates of the Bering Strait inflow based on long-term moorings and summer/autumn ship surveys. The majority of the mooring data are measurements of near-bottom salinity and velocity from up to four sites in the Bering Strait region. Records are available from 1990 to 2004, although not all moorings were deployed every year. Two further effects, both seasonal, also need to be considered: the freshwater of the Alaskan Coastal Current and the

general stratification of the water column in the strait. *Woodgate and Aagaard* [2005] used summer/autumn salinity sections and velocity shear information from a year-round moored Acoustic Doppler Current Profiler from 2000 to 2003 to estimate these terms. They also took advantage of ice draft information from a 1-year mooring to estimate the contribution of sea ice. Combining these various data yields estimated freshwater fluxes for 1990–1992 and 1998–2004.

[37] Environmental challenges have restricted measurement efforts within the Canadian Arctic Archipelago. *Prinsenberg and Hamilton* [2005] collected data from coarsely spaced moorings across a single channel (Lancaster Sound) from 1998 to 2000. Model results that attribute 35–50% of the total Canadian Arctic Archipelago freshwater flux to Lancaster Sound were used to extrapolate these estimates into a proxy for the entire outflow. Farther south, a comparable moored array spanned Davis Strait from 1987–1990 [*Ross*, 1992], allowing a total archipelago discharge to be estimated. The FWI and ASOF programs focus considerable effort on the Canadian Arctic Archipelago beginning in 2004, and new results will emerge in coming years.

[38] On the basis of VEINS/ASOF efforts [e.g., *Ingvaldsen et al.*, 2004; *Schauer et al.*, 2004], *Dickson et al.* [2006] assembled revised estimates of the Atlantic inflow via the West Spitsbergen Current and Barents Sea, relative to a salinity of 35.2. We adopt these values, adjusted to our 34.8 reference. For the Norwegian Coastal Current, we use the value from *Blindheim* [1989].

[39] Model results provide for useful comparisons. The North Atlantic/Arctic Ocean Sea Ice Model (NAOSIM) [*Karcher et al.*, 2005] provides estimates of the Fram Strait liquid outflow. The model was run at 0.25° resolution with 30 levels. NCEP/NCAR (1948–2002) fields provided atmospheric forcing. The PHC climatology (see below) was used for surface restoring at a 180-day timescale. *Karcher et al.* [2005] caution that this restoring dampens surface salinity amplitudes, which might bias freshwater flux estimates. A 1/12° (9 km), 45 vertical level model described by *Maslowski et al.* [2004] provides additional flux estimates. This simulation was forced by ERA-40 data and restored to the PHC surface fields at 30-day timescales. Maslowski provided unpublished results for the present study. Neither model resolves the deformation radius. Transports driven by small-scale recirculations and eddies may thus be poorly characterized. Use is also made of results from *Steele et al.* [1996] and *Zhang and Zhang* [2001].

3.5. Oceanic Freshwater Storage

[40] Liquid freshwater storage in the Arctic Ocean, based on the 34.8 reference, was estimated from salinity profiles contained in the version 3.0 University of Washington Polar Science Center Hydrographic Climatology (PHC) (http://psc.apl.washington.edu/Climatology.html). The PHC uses optimal interpolation to combine data from the 1998 version of the World Ocean Atlas [*Antonov et al.*, 1998; *Boyer et al.*, 1998] with records from the regional Arctic Ocean Atlas [*Environmental Working Group*, 1997, 1998] and selected data from the Bedford Institute of Oceanography. *Steele et al.* [2001] provide an overview of version 2.0. The PHC is only a long-term climatology, with many of the measurements collected in the 1970s. Most are from spring and

summer. Interpolation provides an annual cycle. Estimated errors in freshwater content are 10%. This reflects the sparse hydrographic data and small spatial scales of salinity fields. An alternate method (also used by *Aagaard and Carmack* [1989]), assuming a higher reference of 34.93 (the mean salinity of the deep Arctic Ocean) gives about 15% more freshwater on an annual basis.

[41] Total freshwater storage represents the combination of liquid and sea ice components. Information on the spatial and seasonal distribution of sea ice thickness across the Arctic is sparse. To obtain estimates of the sea ice component, monthly mean sea ice extent was multiplied by an assumed sea ice thickness, with the product adjusted using a density of 900 kg m^{-3} and a salinity of 4. Monthly sea ice extent is based on satellite passive microwave observations over the period 1979–2001, considering all grid cells with at least 15% ice concentration as fully ice covered. A first estimate assumes a uniform ice thickness of 2 m with no annual cycle. A second (reviewed later) includes an annual cycle of ice thickness.

4. Mean Annual View
4.1. Individual Terms

[42] Table 1 summarizes annual means of ERA-40 terms common to both domains (P, ET, P-ET, atmospheric storage). Also provided are observed precipitation from the *Serreze et al.* [2005] data set, and terrestrial ET from CHASM1 and CHASM2. Table 2 provides annual means of ocean fluxes, river input and ocean freshwater storage. Terms are given to two significant digits as yield (mm) and volume (km^3). Values in bold are taken to be the best estimates (see section 4.2). Where available, estimated errors are provided, taken directly from the cited papers, from discussion with their authors or obtained as part of the present effort.

[43] Estimated errors in annual total gauged discharge to the Arctic Ocean from the six largest Eurasian rivers, compiled by *Shiklomanov et al.* [2005] for the period 1950–2000, range from 1.5 to 3.5%. We assume that errors for total Arctic Ocean discharge (from both gauged and ungauged areas, listed separately in Table 2) are represented by the upper end of the estimate. Estimating errors in terms based on ERA-40 and the LSM simulations would be a formidable task, requiring information on errors in the variety of data types assimilated, errors in the forecast model, and errors in the LSM. However, based on comparisons between different reanalyses for the polar cap discussed earlier, it is reasonable to expect errors in aerological P-ET of 10%. Errors in observed precipitation are also very difficult to judge due to spatiotemporal variations in gauge density and uncertainties in bias adjustment procedures. The 20% error assumed here is admittedly little more than a guess and may well be higher.

[44] Looking first at Table 1, precipitation from both observations and ERA-40 is higher over land than ocean. Because of the much larger area of the terrestrial domain, this difference is amplified when means are expressed as km^3. In agreement with *Serreze et al.* [2005], ERA-40 precipitation is somewhat low compared to observations.

[45] Turning to ET, freshwater yield over the Arctic Ocean from ERA-40 of 130 mm is less than half that for

Table 1. Mean Annual Values of Precipitation (P), Evapotranspiration (ET), P-ET, and Atmospheric Water Storage for the Arctic Ocean and Terrestrial Drainage[a]

Budget Term	Ocean,[b] 9.58×10^6 km^2	Land,[b] 15.76×10^6 km^2
Precipitation (P)		
Observed	**340 (3300 ± 680)**	**490 (7700 ± 1500)**
ERA-40	310 (3000)	450 (7100)
Evapotranspiration (ET)		
ERA-40	130 (1200)	300 (4800)
CHASM1	not applicable	250 (3900)
CHASM2	not applicable	200 (3100)
Residual	**140 (1300 ± 710)**	**310 (4800 ± 1500)**
P-ET		
ERA-40, aerological	**210 (2000 ± 200)**	**180 (2900 ± 290)**
ERA-40, forecast	190 (1800)	150 (2300)
Atmospheric water storage		
ERA-40	**7 (63)**	**9 (140)**

    [a]Values are given as both yield (mm) and km^3 (in parentheses), the latter with error estimates where available.
    [b]All terms are based on the period 1979–2001 except observed P and residual ET (both 1979–1993). Residual ET is the difference between observed P and ERA-40 aerological P-ET. Values in bold are considered to be the best estimates (see section 4.2).

land (300 mm). The greater P and ET over land (as yield) implies a more vigorous hydrological cycle. However, pointing to uncertainties, ET over land from ERA-40 is higher than from both CHASM1 (one tile) and CHASM2 (two tile) (recall that the CHASM simulations are driven by ERA-40 inputs). Consistent with findings for the polar cap, both domains show imbalance between the aerologic and forecast estimates of P-ET.

[46] Building on earlier discussion, this imbalance likely relates, at least in part, to model spin-up of the hydrologic cycle. *Betts et al.* [2003] examined this for the Mackenzie. Briefly, at least for this region and in the latter part of the ERA-40 record, the model initial state has too little atmospheric water vapor. Consequently, the model generates too little precipitation over the short-term forecast cycle (the 6-hour forecasts used here). However, given sufficient time (e.g., 36 hours), the model will spin up to restore precipitation. *Betts et al.* [2003] also find that annual ET in ERA-40 is about 30% higher than observations. These results are consistent with lower P-ET from the forecasts, and the observation that ERA-40 precipitation is low compared to observations. The latter conclusion must be viewed in light of uncertainties in the *Legates and Willmott* [1990] adjustments applied to the observations.

[47] *Rothrock et al.* [2000] summarize estimates of the Fram Strait ice volume flux available through the late 1990s. These range from a low of 1600 to a high of 5000 km^3. Assuming an ice density of 900 kg m^{-3}, a salinity of 4 and referencing to a salinity of 34.8, gives a range in the sea ice freshwater flux of 1300 to 4000 km^3. This wide range arises from differences in both record length and measurement techniques. Even the two recent estimates listed in Table 2 from *Kwok et al.* [2004] and *Vinje et al.* [1998] differ by about 500 km^3. The annual mean from the subsequent paper of *Vinje* [2001], based on a longer period (1950–2000), is nearly identical to that of *Vinje et al.* [1998]. The estimate from *Widell et al.* [2003] lies roughly in the middle. The model estimate from Maslowski is considerably lower.

[48] Regarding the upper ocean liquid flux through Fram Strait, most recent sources consider the value from *Aagaard and Carmack* [1989] as too low. *Meredith et al.* [2001] used

two sections of salinity and oxygen isotopes across the passage to examine the ratio of the meteoric water flux to sea ice melt. This was found to be on the order of 2:−1, in agreement with past studies [e.g., *Bauch et al.*, 1995]. Sea ice melt is negative because of net sea ice formation from the waters sampled, not unexpected given the large ice export through Fram Strait.

[49] To correctly interpret this ratio, it is important to appreciate the difference between a meteoric water flux and a net oceanic freshwater flux. The latter includes the effects of both dilution (by river runoff, precipitation and ice melt) and salinification (by sea ice formation). The former, however, includes solely the effects of dilution by river runoff and precipitation. The net oceanic freshwater flux can be estimated from salinity and velocity data alone, while the meteoric flux requires a further tracer (in our case, oxygen isotopes). In the case of liquid fluxes through Fram Strait, one expects the meteoric water flux to be significantly higher than the oceanic freshwater flux, since there is significant southward export of sea ice: the formation of this ice, prior to its export, will reduce the amount of freshwater in the ocean without impacting the meteoric water content. In our case, the 2:−1 ratio observed implies that around half of the diluting effect of meteoric water input is counteracted by brine rejection adding salt to the ocean. Thus the 2:−1 ratio for meteoric water to sea ice melt is approximately equivalent to a 1:1 ratio of oceanic freshwater flux to sea ice flux. Subsequent work [*Taylor et al.*, 2003] confirms this ratio.

[50] *Meredith et al.* [2001] estimated volume transports of meteoric water through Fram Strait of 2000 and 3700 km^3 per year for 1997 and 1998, respectively. Assuming that the meteoric water flux is around twice the net oceanic freshwater flux, these would still convert to values higher than given by *Aagaard and Carmack* [1989]. However, the tracer sections were collected in summer, when the southward flow appears to have its seasonal minimum [see *Fahrbach et al.*, 2001, Figures 5 and 6]. Consequently, based on the velocity field alone, the long-term mean flux should be higher. The value of 2400 km^3 in Table 2 takes this into account. This estimate must be viewed with several strong caveats, in particular, the short record and assumptions of

Table 2. Estimates of Mean Annual Oceanic Freshwater Fluxes, River Input, and Arctic Ocean Freshwater Storage Relative to a Salinity of 34.8[a]

Term	Value, mm	Period of Record
River input		
Gauged (this study)	260 (2500 ± 60)	1980–1999
Gauged plus ungauged (this study)	**330 (3200 ± 110)**	1980–1999
CHASM1 (this study)	310 (3000)	1979–2001 (model)
CHASM2 (this study)	390 (3700)	1979–2001 (model)
ERA-40 (this study)	330 (3200)	1979–2001
Bering Strait inflow		
Woodgate and Aagaard [2005][b]	**260 (2500 ± 300)**	autumn 1990 to summer 2004
Aagaard and Carmack [1989]	180 (1700)	1960s and 1970s
Fram Strait deep outflow		
Dickson et al. [2006]	**50 (500 ± 130)**	not available
Aagaard and Carmack [1989]	19 (180)	not available
Norwegian Coastal Current		
Blindheim [1989]	**26 (250 ± 50)**	not available
Fram Strait ice outflow		
Vinje et al. [1998]	**−240 (−2300 ± 340)**	1990–1996
Kwok et al. [2004]	−190 (−1800 ± 270)	1991–1999
Vinje [2001]	−240 (−2300)	1950–2000
Widell et al. [2003]	−200 (−1900 ± 380)	1996–2000
W. Maslowski (personal communication, 2005)	−170 (−1600)	1979–2002 (model)
Fram Strait upper water outflow		
Meredith et al. [2001]	**−250 (−2400 ± 400)**	1997, 1998
Aagaard and Carmack [1989]	−100 (−1000)	not available
Karcher et al. [2005]	−260 (−2500)	1990–1999 (model)
Karcher et al. [2005]	−220 (−2100)	1948–2002 (model)
W. Maslowski (personal communication, 2005)	−33 (−330)	1979–2002 (model)
Canadian Arctic Archipelago water outflow		
Prinsenberg and Hamilton [2005][c]	**−330 (−3200 ± 320)**	1998–2000+ model
Zhang and Zhang [2001]	−320 (−3100)	model
Steele et al. [1996]	−180 (−1700)	model
Ross [1992][d] and *Cuny et al.* [2005]	−370 (−3500 ± 1900)	1987–1990
W. Maslowski (personal communication, 2005)[d]	−200 (−1900)	1979–2002 (model)
Canadian Arctic Archipelago ice outflow		
Prinsenberg and Hamilton [2005]	**−17 (−160)**	1998–2000
W. Maslowski (personal communication, 2005)	−43 (−410)	1979–2002 (model)
West Spitsbergen Current (Atlantic inflow)		
Dickson et al. [2006]	**−79 (−760 ± 320)**	1997–2000
Aagaard and Carmack [1989]	−17 (−160)	not available
Barents Sea Branch (Atlantic inflow)		
Dickson et al. [2006]	**−35 (−340 ± 80)**	1988–2001
Aagaard and Carmack [1989]	−56 (−540)	not available
Oceanic storage		
Liquid (this study)	**7700 (74000 ± 7400)**	range of years
Sea ice (this study)[e]	**1000 (10000)**	1979–2001
Total	**8700 (84000)**	range of years

[a]Values are given as both yield (mm) and km^3 (in parentheses). Values in bold are taken to be the best estimates. Negative values mean freshwater outflows. Estimated errors are provided where available (also in parentheses).

[b]The period of record is for the "base flow" (from near bottom moorings). The quoted value includes an empirical adjustment for the Alaskan Coastal Current and water column stratification based on data from 2000 to 2003 and the ice flux based on data from 1990 to 1991.

[c]On the basis of 3 years of data in Lancaster Sound, coupled with model information showing that the flux through Lancaster Sound is 35–50% of the total.

[d]Adjusted for Davis Strait.

[e]Assuming a 2.0 m sea ice thickness, salinity of 4, and density of 900 kg m^{-3}.

seasonality. Seasonality is not well defined, and although the total water flux seems to be less in summer, this could be countered by a lower salinity of the flux.

[51] Regarding model estimates, the Fram Strait liquid flux from NAOSIM [*Karcher et al.*, 2005; *Dickson et al.*, 2006] for both 1990–1999 and 1948–2002 is similar to that based on the meteoric water flux. The model estimate from Maslowski is much smaller.

[52] The deep ocean outflow through Fram Strait taken from *Dickson et al.* [2006] is also much larger than that of *Aagaard and Carmack* [1989]. It is based on an estimated water transport of 5 Sv and a salinity of 34.91.

[53] Turning to the Canadian Arctic Archipelago (CAA), recall that the *Prinsenberg and Hamilton* [2005] flux estimate combines 3 years of measurements (1998–2000) across Lancaster Sound with model results. This yields a total annual liquid freshwater flux of 2800 to 3500 km^3. The average value of 3200 km^3 falls close to the modeled value of 3100 km^3 given by *Zhang and Zhang* [2001] while the estimate from *Steele et al.* [1996] is lower, and similar to that of Maslowski. *Prinsenberg and Hamilton* [2005] suggest a small annual sea ice contribution of 160 km^3 compared to the estimate from Maslowski of 410 km^3.

[54] The freshwater flux through Davis Strait can provide another measure of the CAA liquid total. The combined flux through Davis and Hudson Straits represents the integrated CAA outflow after modification from terrestrial runoff and P-ET over Baffin and Hudson Bay. The Ross/Cuny estimate uses the *Cuny et al.* [2005] annual mean freshwater flux of 4100 ± 1900 km^3, adjusted for a Greenland runoff of 570 km^3 [*Dickson et al.*, 2006]. This yields ~3500 km^3, also similar to *Prinsenberg and Hamilton* [2005] and *Zhang and Zhang* [2001]. Although significant freshwater exits Hudson Strait, available estimates are runoff-based [*Loder et al.*, 1998]. We neglect the Hudson Strait component of the CAA freshwater flux (assuming that it is small), which likely biases the total freshwater flux estimate low. Conversely, the *Cuny et al.* [2005] estimates neglect the West Greenland Current (which carries fresh water north) and use rough approximations to account for unmeasured upper ocean salinity structure. These factors may bias the Davis Strait freshwater flux estimates toward large (southward) values.

[55] The Bering Strait inflow from *Woodgate and Aagaard* [2005] of 2500 km^3 is much higher than that cited by *Aagaard and Carmack* [1989]. As discussed, the new value recognizes seasonal transports from the Alaska Coastal Current and seasonal stratification of the water column.

[56] On the basis of the VEINS/ASOF data, the Barents Sea inflow is smaller than estimated by *Aagaard and Carmack* [1989], while the West Spitsbergen current contribution is larger. These new estimates yield a total Atlantic inflow of 1100 km^3 per year.

[57] Gauge records give an annual mean discharge to the Arctic Ocean of 2500 km^3. Adding an estimate for the ungauged part of the drainage (see section 3.3) gives a total of 3200 km^3. ERA-40 also provides its own runoff term that yields the same value. These are within about 10% of P-ET from ERA-40 (2900 km^3). While at face value, this seems like good agreement, our interpretation changes if we consider that, averaged over the terrestrial domain, the imbalance implies an unrealistic loss of 380 mm subsurface water storage over a 20-year period. The CHASM1 discharge value is about 3000 km^3, compared to 3700 km^3 in CHASM2, related to the low ET from this model version. Clearly, the ET is sensitive to the more complex two-tile treatment in CHASM2. By comparison, the difference between the ERA-40 forecasts of P and ET represents a discharge of only 2300 km^3.

[58] Finally, the estimated freshwater storage in the ocean is very large compared to the fluxes. The liquid phase storage of 74,000 km^3 is based on the PHC data set. The sea ice component of 10,000 km^3 is obtained by multiplying an ice thickness of 2.0 m by mean annual ice extent derived from satellite passive microwave observations (see section 3.5). As discussed later, sparse information on ice thickness contributes to large uncertainties in total oceanic freshwater storage.

4.2. Annual Mean Budget

[59] Figure 5 distills the above results into a schematic of the annual mean freshwater budget. The atmospheric box combines the land and ocean domains. The boxes for land and ocean are sized proportional to their relative areas. The width of the arrows is proportional to the size of the transports. The schematic must be viewed with the obvious

caveats that different terms are based on different analysis periods and that some records are very short (see Table 2). Each term is also subject to error, some of which cannot be readily defined. The reference salinity is also involved, as it will be reflected in the sizes of the imports and exports of freshwater.

[60] Starting with the atmosphere, it is apparent that the small storage of water vapor depicted in ERA-40 of about 200 km^3 for the combined land/ocean domain is determined by the difference between large moisture inflows and outflows. On the basis of ERA-40, there is an annual convergence of water vapor into the combined land and ocean domain of 4900 km^3, which can be divided between a P-ET of 2900 km^3 over land, and 2000 km^3 over the ocean. ERA-40 forecasts of P and ET are not in balance with the aerological budget. As outlined earlier, the aerological values of P-ET are considered to provide the better estimates of net water transfers between the atmosphere and surface. While recognizing problems of the sparse gauge network (especially over the Arctic Ocean) and uncertainties in bias adjustments, observed P must still be viewed as the best estimate for this term. Placing faith in observed P and aerological P-ET, the best estimate of ET is taken as the difference between these two terms.

[61] We use the value of river discharge that combines data from the gauge network with estimated contributions for the unmonitored regions (3200 km^3). As mentioned, this value is fairly close to discharge based on ERA-40 aerological P-ET.

[62] For the ocean terms, the most recent estimates are taken to be the most reliable. An exception is the Fram Strait ice flux. The *Vinje et al.* [1998] estimate is preferred over that of *Kwok et al.* [2004] as it better represents summer conditions. It is nearly identical to that of *Vinje* [2001]. *Blindheim's* [1989] value for the Norwegian Coastal Current still appears to be the best available.

[63] Taking the Bering Strait inflow of 2500 km^3 from *Woodgate and Aagaard* [2005] along with the best value of river input (3200 km^3), aerological P-ET for the ocean (2000 km^3), *Blindheim's* [1989] value of 250 km^3 for the Norwegian Coastal Current and the *Dickson et al.* [2006] estimate for the deep ocean Fram Strait transport (500 km^3) yields a total freshwater input to the Arctic Ocean of 8450 km^3. As a percentage of this total, the dominant terms are river runoff (38%), inflow through Bering Strait (30%) and net precipitation (24%). The selected sink terms in Table 2 yield a total outflow of 9160 km^3, dominated by transports through the Canadian Arctic Archipelago (35%) and via Fram Strait as both liquid (26%) and sea ice (25%).

[64] Our results hence indicate ~700 km^3 more freshwater leaving the Arctic Ocean than entering it, equivalent to ~8% of the total estimated inflow. Given errors in the fluxes and very incomplete sampling of interannual variability for some terms, this difference is indistinguishable from zero.

[65] An interesting aspect of the mean annual budget is the vastly different inferred mean residence times of freshwater in the atmosphere and ocean. For the moment assuming steady state, an estimate of residence time can be obtained by dividing annual mean freshwater storage by the sum of the inputs (or the sum of the outputs). Residence time can be interpreted in terms of how long it takes for a change in source terms to affect storage.
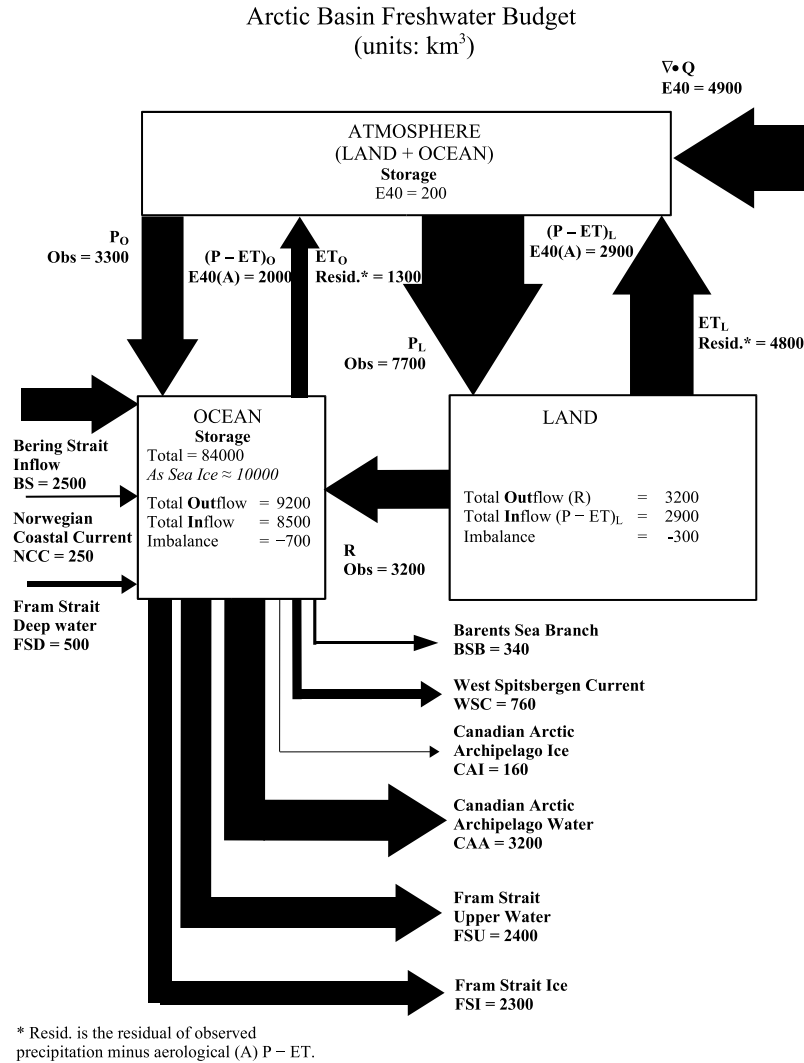
Arctic Basin Freshwater Budget
(units: km^3)

Figure 5. Annual mean freshwater budget of the Arctic. The atmospheric box combines the land and ocean domains. The boxes for land and ocean are sized proportional to their areas. All transports are in units of km^3 per year. Stores are in km^3. The width of the arrows is proportional to the size of the transports. Subscripts "L" and "O" denote land and ocean, respectively. "A" means aerological estimate. See text for further discussion.

[66] For the atmosphere, inputs of the annual vapor flux convergence and the best estimates of ET over land and ocean, yield a mean residence time of about a week, i.e., water cycles very quickly through the atmosphere. A calculation for the ocean, using inputs of precipitation, the Bering Strait inflow, runoff, the Norwegian Coastal Current and the Fram Strait deep outflow (total of 9250 km^3) along with an ocean storage of 84000 km^3 yields a residence time of about a decade. This compares well to the residence time of 11 ± 1 year of Arctic Ocean freshwater using tritium as a tracer [Östlund, 1982], and 6–16 years based on He/tritium ages [Ekwurzel et al., 2001]. Our estimates are also in line with the residence time of about a decade estimated by Aagaard and Coachman [1975], using a very simple freshwater budget.

[67] Data are insufficient to assess mean storages and residence times over land. While information is available for snow water equivalent and near-surface soil moisture,

information would also be needed on water volume locked in permafrost and land ice and stored in lakes and wetlands.

5. Aspects of Variability

5.1. Seasonality

[68] Given sparse information on some key terms, notably the Fram Strait liquid water fluxes and the Canadian Arctic Archipelago throughflow, it is impossible to compile budget schematics by season. However, data are sufficient to examine some aspects of seasonality.

[69] Figure 6a shows mean annual cycles for the ocean domain of P, ET, aerological P-ET and atmospheric storage from ERA-40, based on the period 1979–2001. Corresponding results in Figure 6b use observed P along with ET calculated as a residual from aerological P-ET and observed P (both for 1979–1993). The salient point is that delivery of freshwater to the Arctic Ocean from net precipitation is not spread evenly over the year, but
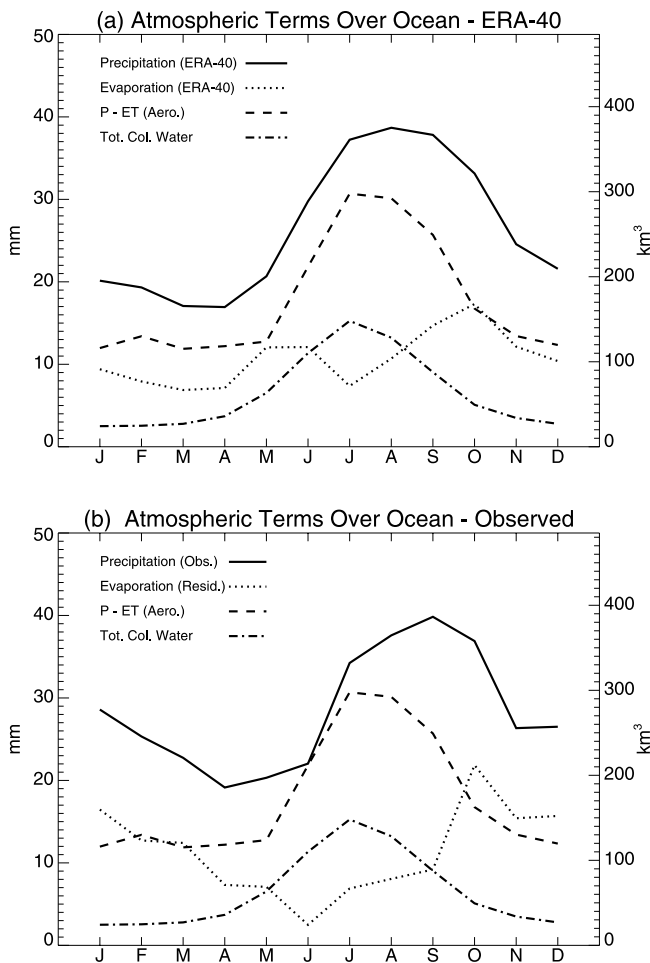
(a) Atmospheric Terms Over Ocean - ERA-40

(b) Atmospheric Terms Over Ocean - Observed

Figure 6. Mean annual cycles for the Arctic Ocean of precipitation (P), evapotranspiration (ET), aerological P-ET, and atmospheric column water vapor. Figure 6a is based on data from the ERA-40 reanalysis over the period 1979–2001. Figure 6b uses observed precipitation and ET calculated as a residual from observed P and aerological P-ET (both for 1979–1993).

peaks in July and is smallest in March. The shape of the annual cycle in P-ET is similar to that of precipitation. The major difference is that precipitation from ERA-40 and observations has a broader July–September peak and is offset more strongly with respect to P-ET through autumn/winter.

[70] Compared to observations, ERA-40 winter precipitation is somewhat low. The July minimum in ET from ERA-40 is consistent with the melting sea ice, which fixes the surface temperature at the freezing point, fostering small vertical vapor gradients. Its rise from July through October makes sense as specific humidity is falling (with cooling of the air) while open water is increasing to a maximum in September (and is still large in October), fostering strong vapor gradients. The atmospheric storage exhibits a fairly symmetric annual cycle, with a minimum in January and maximum in July, following the annual cycle of tropospheric temperatures.

[71] Corresponding results for the terrestrial drainage appear in Figure 7. An interesting feature, noted in earlier

studies [e.g., *Walsh et al.*, 1994; *Serreze et al.*, 2002; *Serreze and Etringer*, 2003] and well expressed here, is that P-ET has a summer minimum, when precipitation is highest. Winter precipitation over the Eurasian drainages (comprising most of our terrestrial drainage) is primarily driven by a modest vapor flux convergence, while the summer peak is largely associated with convective precipitation and strong ET [*Serreze and Etringer*, 2003]. Note that P-ET from the aerological budget is actually slightly negative in July. Imbalances between the aerological and forecast values of P-ET are nevertheless prominent (Figures 7a and 7b). However, as for the ocean domain, the annual cycles of P from ERA-40 and observations are in good agreement, with ERA-40 tending to be slightly low during the cold months. Compared to the ocean, summer ET from ERA-40 is much higher, but there are substantial differences between various land estimates of this term (Figure 8).

[72] Delivery of freshwater from the land to the ocean is strongly modulated by seasonality in snowpack storage and time lags in the routing of snowmelt through river systems. To illustrate these relationships, Figure 9 shows mean
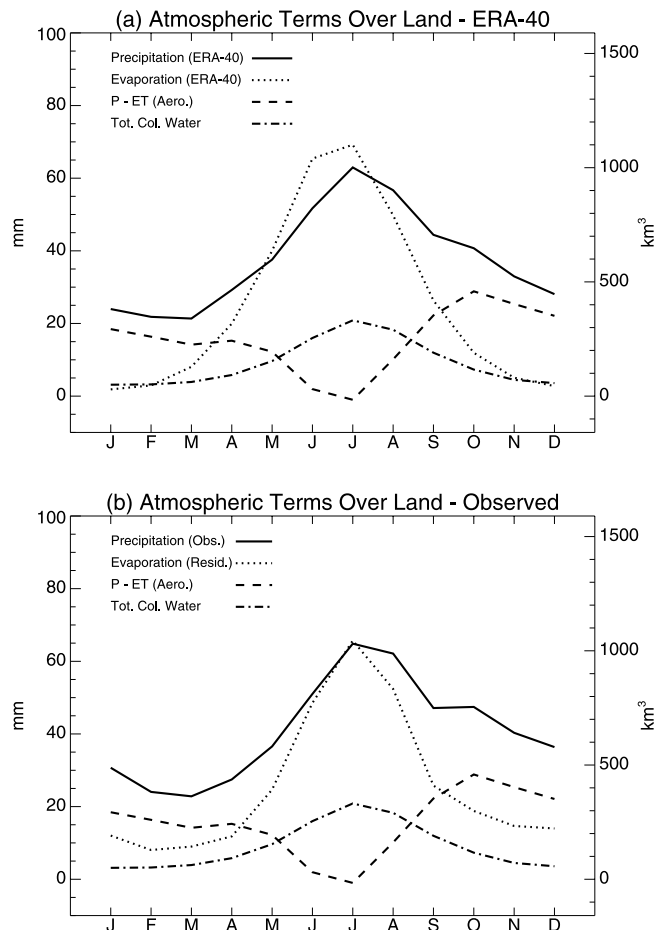

(a) Atmospheric Terms Over Land - ERA-40

(b) Atmospheric Terms Over Land - Observed

Figure 7. Mean annual cycles for the terrestrial drainage of precipitation (P), evapotranspiration (ET), aerological P-ET, and atmospheric column water vapor. Figure 7a is based on data from the ERA-40 reanalysis over the period 1979–2001. Figure 7b uses observed precipitation and ET calculated as a residual from observed P and aerological P-ET (both for 1979–1993).
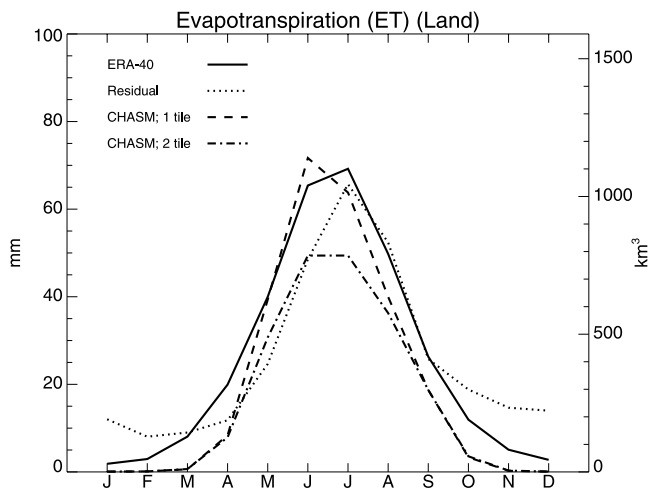
Figure 8. Mean annual cycles (over the period 1979–2001) of evapotranspiration (ET) over the terrestrial drainage from ERA-40, CHASM1, and CHASM2 and calculated as a residual (1979–1993) from observed precipitation and aerological P-ET.

annual cycles of snow water equivalent (SWE) from ERA-40, CHASM1 and CHASM2, along with runoff from CHASM1, CHASM2 and the gauge network (the latter including estimates for the ungauged regions). We stress that CHASM has no river routing; runoff is simply the sum of runoff from all grid cells in the domain.

[73] The annual cycle of SWE from the two CHASM runs is essentially identical, i.e., the two lines in Figure 9 lie atop each other, and is similar to that from ERA-40. This is expected, given that the snowpack for all three cases
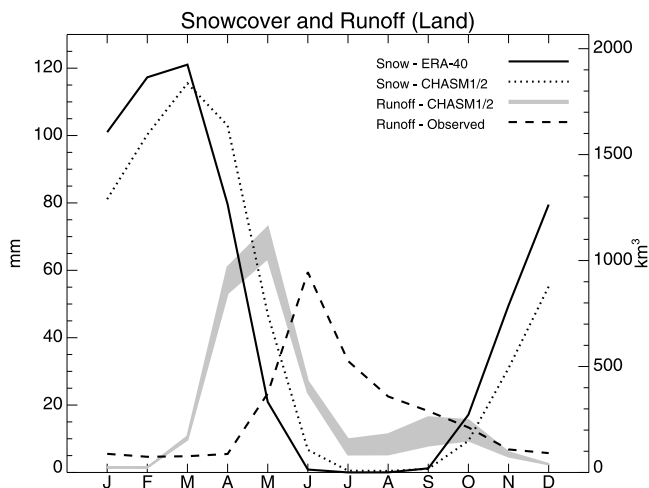
depends, in part, on ERA-40 precipitation and temperature. For most of the year, P-ET is stored as snow. The snowpack begins to build between September and October, reaching a maximum in March. The SWE then decreases sharply through spring. Part of spring melt replenishes the soil moisture store, but the bulk appears as runoff. CHASM1 and CHASM2 show a strong May peak in runoff, dropping sharply through June. Illustrating time lags in routing water through river systems, the delivery of snowmelt to the Arctic Ocean seen in the gauge-based runoff, occurs a month later in June.

[74] Turning to the ocean flux terms for which data are sufficient, Figure 10 summarizes mean annual cycles of the Fram Strait ice outflow from *Vinje et al.* [1998] and *Kwok et al.* [2004], along with the mean annual cycle of the Bering Strait inflow. *Vinje et al.* [1998] gives larger Fram Strait fluxes in all months. Identical means from June to September in the *Kwok et al.* [2004] data set are explained in that they only provided sums over these four months based on regression techniques (see section 3.4). Freshwater export to the Atlantic from ice is largest in winter, due to generally thick ice and to strong winds. The smaller flux in summer points to smaller ice thickness, as well as weaker winds [*Vinje*, 2001].

[75] This seasonality is in sharp contrast to that for the Bering Strait inflow, which features a general summer maximum and a June peak. This annual cycle was compiled by first taking the climatology of the baseline transport from *Woodgate and Aagaard* [2005], using the near-bottom mooring data collected over 1990–2004. Contributions from the Alaskan Coastal Current (ACC) were then estimated from one year of data. The ACC annual freshwater transport (220–240 km^3) appears to be present for eight months (May through December) [*Woodgate and Aagaard*, 2005]. We assumed seasonality in the ACC freshwater transport matching that of Yukon River discharge (a probable source of freshwater for the ACC), but lagged by one
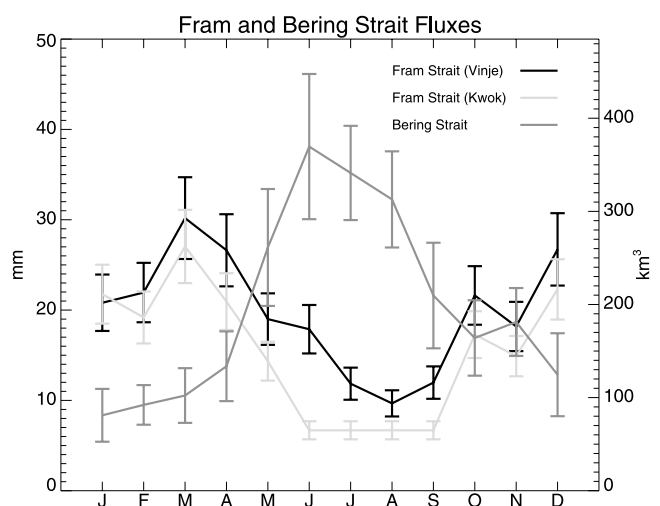

Figure 9. Mean annual cycles of snowpack storage from ERA-40, CHASM1, and CHASM2, along with runoff from CHASM1, CHASM2 (bottom and top boundaries of shaded area), and observations (gauged plus estimated contributions for the ungauged area). CHASM output is for the period 1979–2001. Gauged runoff is for the period 1980–1999.

Figure 10. Mean annual cycles (with error bars) of the Fram Strait ice outflow from *Vinje et al.* [1998] and *Kwok et al.* [2004], along with the mean annual cycle of the Bering Strait inflow based on *Woodgate and Aagaard* [2005]. Records lengths are variable.
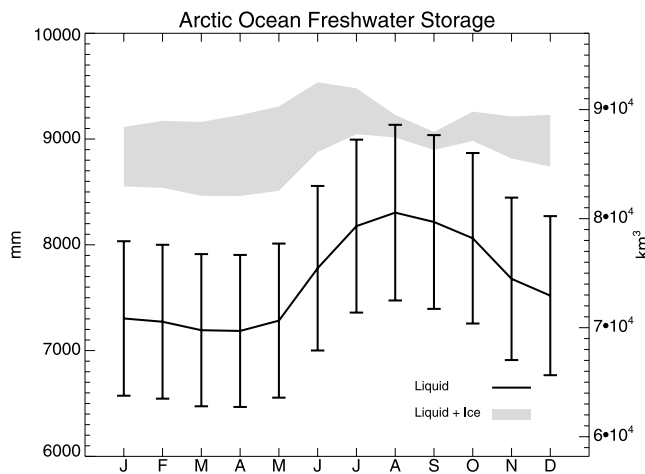
Figure 11. Mean annual cycles of freshwater storage in the Arctic Ocean based on the liquid portion only (from the PHC, solid line with estimated error bars) and for liquid plus ice (total storage) using observed ice area with a 2 m ice thickness (bottom boundary of shaded area) and using observed ice area with a modeled annual cycle of ice thickness (top boundary of shaded area). Errors in total storage are not known but must be very large.

month, a reasonable transit time from the Yukon to Bering Strait. To this, we added an estimated effect of seasonal variations in the salinity profile (seasonal stratification) based on summer/autumn hydrographic data. Ice transport through the strait was neglected as small compared to other uncertainties While the results in Figure 10 must be viewed in light of uncertainties in the ACC and seasonal stratification, the annual cycle of the mean baseline freshwater transport has the same basic shape as shown in Figure 10. The ACC and seasonal stratification serve to amplify the summer peak.

[76] The general spring to summer increases in runoff, P-ET over the Ocean and the Bering Strait inflow will collectively contribute to a spring-summer increase in freshwater storage. The spring through summer decline in the Fram Strait ice outflow should amplify this effect. Seasonality in other large terms is not well known. Limited

data suggest that the Canadian Arctic Archipelago freshwater transport peaks in late summer [*Prinsenberg and Hamilton*, 2005; *Cuny et al.* 2005], which would have a countering effect.

[77] Can seasonal changes in fluxes be discerned in the annual cycle of Arctic Ocean freshwater storage? Figure 11 provides three estimates of the annual cycle in storage. The first is the liquid component from the PHC records. These data show a pronounced increase between May (71000 km^3) to a maximum of 81000 km^3 in August, a change of 10000 km^3, followed by autumn decline. The May–August increase is larger than the total annual inputs to the Arctic Ocean, and dwarfs combined seasonal changes in the fluxes shown in Figure 10. It is therefore likely that the annual cycle from the PHC records is dominated by phase change, i.e., seasonal transfers of freshwater from the solid to liquid phase in spring and summer, and vice versa from autumn through winter.

[78] What is wanted is the change in total freshwater storage (liquid and ice). As one estimate, we add to the liquid component monthly values of the sea ice component based on satellite-derived sea ice extent, a constant 2 m ice thickness, a salinity of 4 and a density of 900 kg m^{-3} (see section 3.5). The resulting annual cycle is much less pronounced. Another estimate combines ice extent with an annual cycle of ice thickness, based on an updated version of the *Schramm et al.* [1997] single-column model (with 40 ice thickness categories) summarized by *Steele and Flato* [2000]. The modeled ice thickness ranges from 3.3 m in May to 2.5 m in September. Given the greater ice thicknesses from the latter estimate, the total storage is larger, but the annual cycle in total storage also changes shape with a June maximum.

[79] While the suggested general summer maximum in Arctic Ocean total freshwater storage is intriguing, uncertainties in the available data obscure the effect of freshwater flux seasonality. This is understood in that (1) the estimated 10% error on the PHC-derived liquid storage component exceeds the magnitude of seasonal flux variations and is similar in size to the total annual freshwater input to the Arctic Ocean, (2) even fluxes for which seasonal information is available have large errors, and (3) there are insufficient data on ice volume to obtain accurate estimates of total storage. Accordingly, attempts to relate the com-

Table 3. Mean, Range, Standard Deviation, and Coefficient of Variation for Annual Freshwater Fluxes

Variable	Mean, km^3 yr^{-1}	Range, km^3 yr^{-1}	Standard Deviation	Coefficient of Variation[a]	Period of Record
River discharge					
Gauged	2500	470	114	0.05	1980–1999
Gauged plus ungauged	3200	429	120	0.04	1980–1999
P-ET					
Ocean, ERA-40	2000	760	170	0.09	1979–2001
Land, ERA-40	2900	620	160	0.06	1979–2001
Fram Strait ice flux					
Vinje et al. [1998]	2400	1300	610	0.25	1991–1995
Vinje [2001]	2300	—	530	0.23	1950–2000
Kwok et al. [2004]	1800	670	280	0.16	1992–1998
Bering Strait inflow					
Woodgate and Aagaard [2005][b]	2500	700	270	0.11	1991, 1992, 1998–2004

[a]Standard deviation divided by the mean.
[b]Not accounting for interannual variability of stratification, Alaskan Coastal Current, or sea ice.
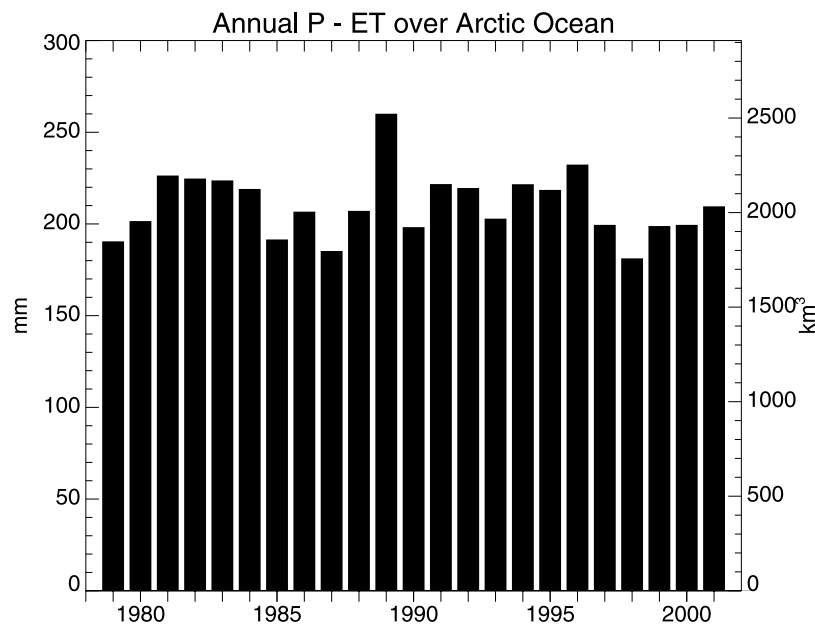
Figure 12. Annual time series of aerological P-ET from ERA-40 for the ocean domain.

bined annual cycle of the relative unknowns (Fram Strait liquid outflow, the CAA outflow, the Norwegian Coastal Current and the Atlantic inflow) to monthly changes in estimated total freshwater storage are meaningless.

5.2. Interannual Variability

[80] Available data can also only draw a very incomplete picture of interannual variability. Table 3 summarizes the mean, range, standard deviation and coefficient of variation (standard deviation divided by the mean) of major flux terms for which time series are available. The mean for the Fram Strait outflow from *Vinje et al.* [1998] is slightly different than in Table 2 as the analysis is limited to just the years for which data are available for all months.

[81] Figure 12 shows the annual P-ET time series for the ocean domain (1979–2001). There is no obvious trend. The standard deviation is 170 km^3, yielding a rather low coefficient of variation (0.09). The standard deviation and coefficient of variation of P-ET is also small for land. This follows, since P-ET is aggregated over very large domains; regional anomalies tend to get averaged out. The smaller variability over the land domain is consistent with its larger area. Variability in river discharge is hence also small. There is only broad correspondence between the time series of terrestrial P-ET and discharge (Figure 13). This points to land surface or subsurface storage. Over the period 1936–1999, *Peterson et al.* [2002] document a positive trend (a 7% total change, equating to about 130 km^3) in aggregate annual discharge from the six largest Eurasian rivers. Our results, based on a shorter record that includes discharge from the Mackenzie, show no obvious trend. However, for reasons still unclear, runoff from CHASM1 and CHASM2, also shown in Figure 13, has a slight downward tendency over the period of record.

[82] Although based on only 9 years of data, the Bering Strait inflow seems more variable than P-ET and river discharge (Table 3). The real variability is likely greater, since corrections for the Alaskan Coastal Current and

seasonal stratification, while taken as constant, probably vary from year to year [*Woodgate et al.*, 2005a]. Of note (but not shown) is the comparatively large inflow (2900 km^3) for the last 2 years for the record (2003 and 2004) [*Woodgate and Aagaard*, 2005].

[83] Turning to the Fram Strait ice outflow, there are considerable differences between the statistics from *Vinje et al.* [1998] and *Kwok et al.* [2004] (see also Table 4). However, the standard deviation (530 km) and coefficient of variation (0.23) from the longer record of *Vinje* [2001] are substantially larger than P-ET over the ocean, runoff, and the Bering Strait inflow.

[84] In summary, it appears that of the flux terms for which information is available, the Fram Strait ice outflow plays a relatively strong role in contributing to interannual variability in the freshwater budget. This is not surprising given the sensitivity of the flux to the regional wind field. In an earlier study focusing on the cold season, *Kwok and Rothrock* [1999] document positive trends in Fram Strait ice area and volume fluxes from the late 1970s through much of the 1990s in association with a positive shift in the index of the North Atlantic Oscillation (NAO). As the NAO turned positive, there was a shift in the wind fields in the vicinity of Fram Strait that would promote a larger ice flux. However, no such trend for this period is evident in the annual time series of *Vinje* [2001] (his Figure 2), although it does indicate an increase in the volume flux from about 1990 to 1996, followed by a general decline.

6. Summary and Conclusions

[85] Recent work [*Woodgate and Aagaard*, 2005] has helped to constrain the Bering Strait inflow. Compared to earlier estimates [*Aagaard and Carmack*, 1989] this term has grown in importance as a freshwater source to the Arctic Ocean. Aerological P-ET from the ERA-40 reanalysis appears to give a reasonable accounting of the atmospheric branch of the system. River input is also reasonably well
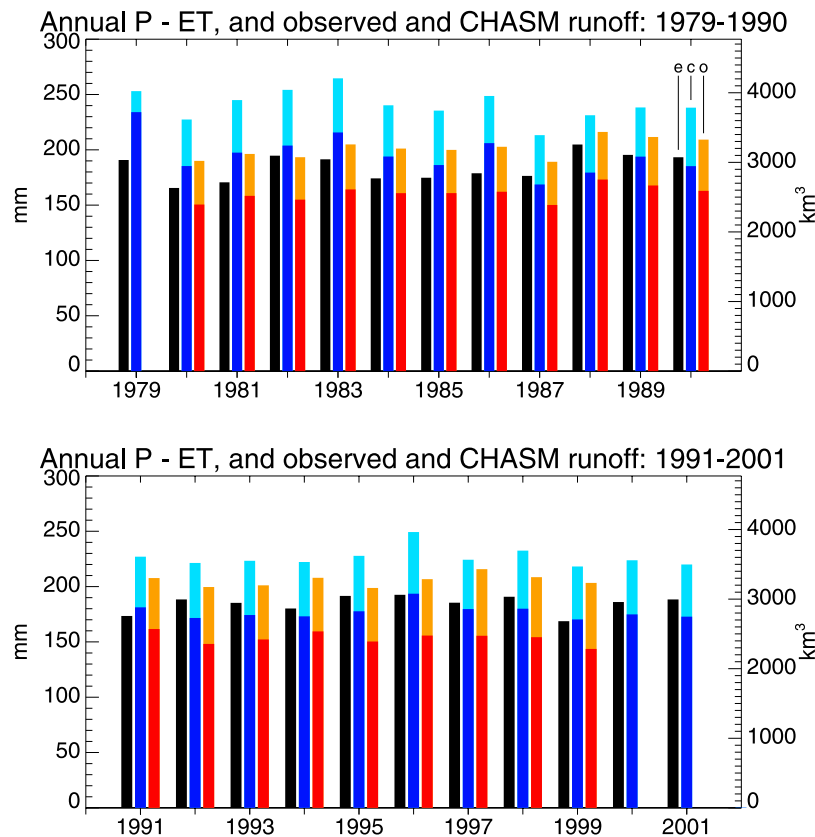
Figure 13. Time series of annual P-ET from ERA-40 for the land domain (black shading, bar e); annual runoff from CHASM 1 (dark blue shading, bar c) and CHASM 2 (light blue shading, bar c); annual river input to the Arctic Ocean based on the gauge network (red shading, bar o); and the ungauged part of the terrestrial drainage (orange shading, bar o).

defined. This is supported by agreement (to about 10%) between annual mean runoff and aerological P-ET over the terrestrial drainage. The individual terms P and ET comprising net precipitation are by contrast less certain, seen, for example, in disparity between ET estimates from ERA-40 and two versions of the CHASM model.

[86] Satellite and ULS data have provided new estimates of the Fram Strait ice outflow. However, recent values still range widely. Large uncertainties remain regarding liquid fluxes through the Canadian Arctic Archipelago and Fram Strait, as well as the components of Atlantic inflow. Nevertheless, it now appears that the liquid freshwater export through Fram Strait is as large as the transport via sea ice, helping to balance the upward revision in the Bering Strait inflow. In all the straits, much of the liquid freshwater moves in a near-surface layer where the potential for collisions with ice keels prevents the use of conventional moored instrumentation. Strong boundary currents flowing over the Baffin and Greenland shelves likely carry a significant portion of the freshwater flux, but difficulties in taking measurements over these shallow, ice-threatened regions have impeded efforts to further quantify their contributions. Last, the critical straits are typically wide relative to the local internal deformation radius and thus admit small-scale circulation features which complicate interpretation of coarsely spaced measurements.

[87] On the basis of a reference salinity of 34.8 and taking the best estimates of different terms, we find that freshwater input to the Arctic Ocean is dominated by river runoff (38%), inflow through Bering Strait (30%) and net precipitation over the Arctic Ocean itself (24%). Total freshwater export from the Arctic Ocean to the North Atlantic is dominated by transports through the Canadian Arctic Archipelago (35%) and via Fram Strait as both liquid (26%) and sea ice (25%). The difference between annual mean oceanic outflows and inflows is indistinguishable from zero when errors are considered. Given measurement errors, incomplete sampling of interannual variability, and recog-

Table 4. Annual Values of the Fram Strait Freshwater Outflow as Sea Ice From *Vinje et al.* [1998] and *Kwok et al.* [2004][a]

	Year								
	1991	1992	1993	1994	1995	1996	1997	1998	1999
Vinje et al. [1998]	1800	2200	2000	3100	3000	NA	NA	NA	NA
Kwok et al. [2004]	NA	1600	1500	2300	2100	1700	1700	1700	NA

[a]NA means not available. Values are in km³ yr⁻¹.

nizing that the system is likely never in a steady state, this is probably fortuitous. In agreement with previous studies, the estimated mean residence time of freshwater in the Arctic Ocean is about a decade. This contrasts sharply with the atmosphere, where the residence time of freshwater is roughly a week.

[88] Only limited statements can be made regarding seasonal and interannual variability. Prominent seasonality is evident in runoff, P-ET over the Arctic Ocean, the Bering Strait inflow and the Fram Strait ice flux, while the Fram Strait ice outflow appears to have the largest interannual variability. However, recent modeling work suggests that variability in Arctic Ocean freshwater content is driven most strongly by changes in the Atlantic inflow [*Häkkinen and Proshutinsky*, 2004]. Our study points to great uncertainty in the annual cycle of total freshwater storage in the Arctic Ocean, due in part to uncertainties in the liquid portion but especially sea ice volume. These uncertainties overwhelm storage changes associated with seasonality in freshwater fluxes.

[89] In conclusion, it seems that despite years of research, ranging from the pioneering efforts of *Mosby* [1962], *Aagaard and Greisman* [1975], *Östlund and Hut* [1984], and *Aagaard and Carmack* [1989] to the wealth of recent studies over the past decade, which increasingly are driven by the recognition that the Arctic atmosphere, land surface, and ocean are in the midst of pronounced change [*Arctic Climate Impact Assessment*, 2005], our understanding of the Arctic freshwater system is still far from complete. How does this fascinating, intimately coupled system fit into the broader picture of Arctic change? Is it a passive responder, or an active driver of change? Answering these questions promises to be at the forefront of Arctic research in coming decades.

References

Aagaard, K., and E. C. Carmack (1989), The role of sea ice and other fresh waters in the Arctic circulation, *J. Geophys. Res.*, *94*(C10), 14,485–14,498.

Aagaard, K., and L. K. Coachman (1975), Toward an ice-free Arctic Ocean, *Eos Trans. AGU*, *56*, 484–486.

Aagaard, K., and P. Greisman (1975), Toward new mass and heat budgets for the Arctic Ocean, *J. Geophys. Res.*, *80*, 3821–3827.

Aagaard, K., and R. A. Woodgate (2001), Some thoughts on the freezing and melting of sea ice and their effects on the ocean, *Ocean Modell.*, *3*, 127–135.

Aagaard, K., A. T. Roach, and J. D. Schumacher (1985), On the wind-driven variability of the flow through Bering Strait, *J. Geophys. Res.*, *90*, 7213–7221.

Aagaard, K., E. Farhbach, J. Meincke, and J. H. Swift (1991), Saline outflow from the Arctic Ocean: Its contribution to the deep waters of the Greenland, Norwegian and Iceland seas, *J. Geophys. Res.*, *96*, 20,433–20,441.

Antonov, J. I., S. Levitus, T. P. Boyer, M. E. Conkright, T. D. O'Brien, and C. Stephens (1998), *World Ocean Atlas 1998*, vol. 1, *Temperature of the Atlantic Ocean*, NOAA Atlas NESDIS 27, 166 pp., NOAA, Silver Spring, Md.

Arctic Climate Impact Assessment (2005), *Impacts of a Warming Climate: Arctic Climate Impact Assessment*, Cambridge Univ. Press, New York.

Bauch, D., P. Schlosser, and R. D. Fairbanks (1995), Freshwater balance and the sources of deep and bottom waters in the Arctic Ocean inferred from the distribution of H_2 ^{18}O, *Prog. Oceanogr.*, *35*, 53–80.

Betts, A. K., J. H. Ball, and P. Viterbo (2003), Evaluation of the ERA-40 surface water budget and surface temperature for the Mackenzie river basin, *J. Hydrometeorol.*, *4*, 1194–1211.

Blindheim, J. (1989), Cascading of Barents Sea bottom water into the Norwegian Sea, *Rapp. P. V. Reun. Cons. Int. Exp. Mer.*, *188*, 49–58.

Boyer, T. P., S. Levitus, J. I. Antonov, M. E. Conkright, T. D. O'Brien, and C. Stephens (1998), *World Ocean Atlas 1998*, vol. 4, *Salinity of the Atlantic Ocean*, NOAA Atlas NESDIS 30, 166 pp., NOAA, Silver Spring, Md.

Carmack, E. C. (2000), The Arctic Ocean's freshwater budget: Sources, storage and export, in *The Freshwater Budget of the Arctic Ocean*, edited by E. L. Lewis et al., pp. 91–126, Springer, New York.

Cavalieri, D. J., C. L. Parkinson, and K. Y. Vinnikov (2003), 30-year satellite records reveal contrasting Arctic and Antarctic decadal sea ice variability, *Geophys. Res. Lett.*, *30*(18), 1970, doi:10.1029/2003GL018031.

Coachman, L. K., and K. Aagaard (1966), On the water exchange through Bering Strait, *Limnol. Oceanogr.*, *11*, 44–59.

Coachman, L. K., and K. Aagaard (1981), Re-evaluation of water transports in the vicinity of Bering Strait, in *The Eastern Bering Sea Shelf: Oceanography and Resources*, vol. 1, edited by D. W. Hood and J. A. Calder, pp. 95–110, NOAA, Silver Spring, Md.

Cullather, R. I., D. H. Bromwich, and M. C. Serreze (2000), The atmospheric hydrologic cycle over the Arctic basin from reanalyses. Part I: Comparisons with observations and previous studies, *J. Clim.*, *13*, 923–937.

Cuny, J., P. B. Rhines, and R. Kwok (2005), Davis Strait volume, freshwater and heat fluxes, *Deep Sea Res., Part I*, *52*, 519–542.

Curry, R., and C. Mauritzen (2005), Dilution of the northern North Atlantic Ocean in recent decades, *Science*, *308*, 1772–1774.

Deardorff, J. W. (1978), Efficient prediction of ground surface temperature and moisture, with inclusion of a layer of vegetation, *J. Geophys. Res.*, *83*, 1889–1903.

Desborough, C. E. (1999), Surface energy balance complexity in GCM land surface models, *Clim. Dyn.*, *15*, 389–403.

Dickson, R. R., J. Meincke, S. A. Malmberg, and J. Lee (1988), The "Great Salinity Anomaly" in the northern North Atlantic 1968–1982, *Prog. Oceanogr.*, *20*, 103–151.

Dickson, R., S. Dye, M. Karcher, J. Meincke, B. Rudels, and I. Yashayaev (2006), Current estimates of freshwater flux through Arctic and subarctic seas, *Prog. Oceanogr.*, in press.

Dirmeyer, P. A., A. J. Dolman, and N. Sato (1999), The pilot phase of the Global Soil Wetness Project, *Bull. Am. Meteorol. Soc.*, *80*, 851–878.

Dukhovskoy, D. S., M. A. Johnson, and A. Proshutinsky (2004), Arctic decadal variability: An auto-oscillatory system of heat and fresh water exchange, *Geophys. Res. Lett.*, *31*, L03302, doi:10.1029/2003GL019023.

Ekwurzel, B. P., P. Schlosser, R. A. Mortlock, and R. G. Fairbanks (2001), River runoff, sea ice meltwater, and Pacific water distribution and mean residence times in the Arctic Ocean, *J. Geophys. Res.*, *106*, 9075–9092.

Environmental Working Group (1997), *Joint U.S.-Russian Atlas of the Arctic Ocean for the Winter Period* [CD-ROM], Natl. Snow and Ice Data Cent., Boulder, Colo.

Environmental Working Group (1998), *Joint U.S.-Russian Atlas of the Arctic Ocean for the Summer Period* [CD-ROM], Natl. Snow and Ice Data Cent., Boulder, Colo.

Fahrbach, E., J. Meinske, S. Osterhus, G. Rohardt, U. Schauer, V. Tveberg, and J. Verduin (2001), Direct measurements of volume transports through Fram Strait, *Pol. Res.*, *20*, 217–224.

Genthon, C. (1998), Energy and moisture flux across 70°N and S from ECMWF re-Analysis, in *Proceedings of First WCRP International Conference on Reanalyses*, Rep. WCRP-104 9WMO/TD 876, pp. 371–374, World Meteorol. Organ., Geneva, Switzerland.

Gober, M., P. Hagenbrock, F. Ament, and A. Hense (2003), Comparing mass-consistent atmospheric moisture budgets on an irregular grid: An Arctic example, *Q. J. R. Meteorol. Soc.*, *129*, 2383–2400.

Gudkovich, Z. M. (1962), On the nature of the Pacific current in Bering Strait and the causes of its seasonal variations, *Deep Sea Res.*, *9*, 507–510.

Häkkinen, S. (1999), A simulation of the thermohaline effects of a Great Salinity Anomaly, *J. Clim.*, *12*, 1781–1795.

Häkkinen, S., and A. Proshutinsky (2004), Freshwater content variability in the Arctic Ocean, *J. Geophys. Res.*, *109*, C03051, doi:10.1029/2003JC001940.

Hanzlick, D. J. (1983), The West Spitsbergen Current: Transport, forcing, and variability, Ph.D. dissertation, 127 pp., Univ. of Wash., Seattle.

Holland, M. M., C. M. Bitz, M. Eby, and A. J. Weaver (2001), The role of ice-ocean interactions in the variability of the North Atlantic thermohaline circulation, *J. Clim.*, *14*, 656–675.

Ingvaldsen, R. B., L. Asplin, and H. Loeng (2004), The seasonal cycle in the Atlantic transport to the Barents Sea during the years 1997–2001, *Cont. Shelf Res.*, *24*, 1015–1032.

Jonsson, S. (1989), The structure and forcing of the large-and mesoscale circulation in the Nordic Seas, with special reference to the Fram Strait, Ph.D. dissertation, 144 pp., Univ. of Bergen, Bergen, Norway.

Karcher, M., R. Gerdes, F. Kauker, C. Koberle, and I. Yashayaev (2005), Arctic Ocean change heralds North Atlantic freshening, *Geophys. Res. Lett.*, *32*, L21606, doi:10.1029/2005GL023861.

Kwok, R., and D. A. Rothrock (1999), Variability of Fram Strait ice flux and North Atlantic Oscillation, *J. Geophys. Res.*, *104*, 5177–5189.

Kwok, R., G. F. Cunningham, and S. S. Pang (2004), Fram Strait ice outflow, *J. Geophys. Res.*, *109*, C01009, doi:10.1029/2003JC001785.

Kwok, R., W. Maslowski, and S. W. Laxon (2005), On large outflows of Arctic sea ice into the Barents Sea, *Geophys. Res. Lett.*, *32*, L22503, doi:10.1029/2005GL024485.

Lammers, R. B., A. I. Shiklomanov, C. J. Vorosmarty, B. M. Fekete, and B. J. Peterson (2001), Assessment of contemporary Arctic river runoff from observational records, *J. Geophys. Res.*, *106*, 3321–3334.

Legates, D. R., and C. J. Willmott (1990), Mean seasonal and spatial variability in gauge-corrected, global precipitation, *Int. J. Climatol.*, *10*, 111–127.

Loder, J. W., B. Petrie, and G. Gawarkiewicz (1998), The coastal ocean off northeastern North America: A large scale view, in *The Sea*, vol. 11, *The Global Coastal Ocean: Regional Studies and Syntheses*, edited by A. R. Robinson and K. H. Brink, pp. 105–133, John Wiley, Hoboken, N. J.

Manabe, S. (1969), Climate and the ocean circulation. 1. The atmospheric circulation and the hydrology of the Earth's surface, *Mon. Weather Rev.*, *97*, 739–777.

Maslowski, W., D. Marble, W. Walczowski, U. Schauer, J. L. Clement, and A. J. Semtner (2004), On climatological mass, heat and salt transports through the Barents Sea and Fram Strait from a Pan-Arctic coupled ice-ocean model simulation, *J. Geophys. Res.*, *109*, C03032, doi:10.1029/2001JC001039.

Meredith, M. P., K. Heywood, P. Dennis, L. Goldson, R. White, E. Fahrbach, U. Schauer, and S. Osterhus (2001), Freshwater fluxes through the western Fram Strait, *Geophys. Res. Lett.*, *28*, 1615–1618.

Mosby, H. (1962), Water, salt and heat balance of the north Polar Sea and of the Norwegian Sea, *Geofys. Publ.*, *24*, 289–313.

Nakamura, M., and A. H. Oort (1988), Atmospheric heat budgets of the polar regions, *J. Geophys. Res.*, *93*, 9510–9524.

Östlund, H. G. (1982), The residence time of the freshwater component in the Arctic Ocean, *J. Geophys. Res.*, *87*, 2035–2043.

Östlund, H. G., and G. Hut (1984), Arctic Ocean water mass balance from isotope data, *J. Geophys. Res.*, *89*, 6373–6381.

Peterson, B. J., R. M. Holmes, J. W. McClelland, C. J. Vorosmarty, R. B. Lammers, A. I. Shiklomanov, I. A. Shiklomanov, and S. Rahmstorf (2002), Increasing river discharge to the Arctic Ocean, *Science*, *298*, 2171–2173.

Prinsenberg, S. J., and J. Hamilton (2005), Monitoring the volume, freshwater and heat fluxes passing through Lancaster Sound in the Canadian Arctic Archipelago, *Atmos. Ocean*, *43*, 1–22.

Proshutinsky, A., R. H. Bourke, and F. A. McLaughlin (2002), The role of the Beaufort Gyre in Arctic climate variability: Seasonal to decadal climate scales, *Geophys. Res. Lett.*, *29*(23), 2100, doi:10.1029/2002GL015847.

Rignot, E., S. P. Gogineni, I. Joughin, and W. B. Krabill (2001), Contribution to the glaciology of northern Greenland from satellite radar interferometry, *J. Geophys. Res.*, *106*, 34,007–34,020.

Ross, C. (1992), Moored current meter measurements across Davis Strait, *Res. Doc. 92/70*, Northwest Atlantic Fish. Organ., Dartmouth, N. S., Canada.

Rothrock, D. A., Y. Yu, and G. A. Maykut (1999), Thinning of the Arctic sea ice cover, *Geophys. Res. Lett.*, *26*, 3469–3472.

Rothrock, D. A., R. Kwok, and D. Groves (2000), Satellite views of the Arctic freshwater balance, in *The Freshwater Budget of the Arctic Ocean*, edited by E. L. Lewis et al., pp. 409–451, Springer, New York.

Rudels, B., E. P. Jones, L. G. Anderson, and G. Kattner (1994), On the intermediate depth waters of the Arctic Ocean, in *The Polar Oceans and Their Role in Shaping the Global Environment*, *Geophys. Monogr. Ser.*, vol. 85, edited by O. M. Johannessen, R. D. Muench, and J. E. Overland, pp. 33–46, AGU, Washington, D. C.

Schauer, U., E. Fahrbach, S. Osterhus, and G. Rohardt (2004), Arctic warming through the Fram Strait: Oceanic heat transport from 3 years of measurements, *J. Geophys. Res.*, *109*, C06026, doi:10.1029/2003JC001823.

Schramm, J. L., M. M. Holland, and J. A. Curry (1997), Modeling the thermodynamics of a sea ice thickness distribution: 1. Sensitivity to ice thickness resolution, *J. Geophys. Res.*, *102*, 23,079–23,091.

Serreze, M. C., and A. J. Etringer (2003), Precipitation characteristics of the Eurasian Arctic drainage system, *Int. J. Climatol.*, *23*, 1267–1291.

Serreze, M. C., R. G. Barry, and J. E. Walsh (1995), Atmospheric water vapor characteristics at 70°N, *J. Clim.*, *8*, 719–731.

Serreze, M. C., D. H. Bromwich, M. P. Clark, A. J. Etringer, T. Zhang, and R. Lammers (2002), The large-scale hydro-climatology of the Arctic drainage, *J. Geophys. Res.*, *107*, 8160, doi:10.1029/2001JD000919. (Printed *108*(D2), 2003.)

Serreze, M. C., A. Barrett, and F. Lo (2005), Northern high latitude precipitation as depicted by atmospheric reanalyses and satellite retrievals, *Mon. Weather Rev.*, *133*, 3407–3430.

Shiklomanov, A. I., R. B. Lammers, and C. J. Vörösmarty (2002), Widespread decline in hydrological monitoring threatens pan-Arctic research, *Eos Trans. AGU*, *83*, 13,16, 17.

Shiklomanov, A. I., T. I. Yakovleva, R. B. Lammers, I. P. Karasev, C. J. Vörösmarty, and E. Linder (2005), Cold region river discharge uncertainty: Estimates from large Russian rivers, *J. Hydrol.*, *326*(1–4), 231–256.

Shtokman, V. B. (1957), Vliyanie vetra na techeniya v Beringovo Prolive, prichiny ikh bol'shikh skorostei i preobladayueshego severnogo napravleniya, *Tr. Inst. Okeanolog. Akad. Nauk SSSR*, *25*, 171–197.

Slater, A. G., et al. (2001), The representation of snow in land-surface schemes: Results from PILPS 2(d), *J. Hydrometeorol.*, *2*, 7–25.

Steele, M., and G. M. Flato (2000), Sea ice growth, melt, and modeling, in *The Freshwater Budget of the Arctic Ocean*, edited by E. L. Lewis et al., pp. 549–587, Springer, New York.

Steele, M., D. Thomas, D. Rothrock, and S. Martin (1996), A simple model study of the Arctic Ocean freshwater balance, 1979–1985, *J. Geophys. Res.*, *101*, 20,833–20,848.

Steele, M., R. Morley, and W. Ermold (2001), PHC: A global ocean hydrography with a high-quality Arctic Ocean, *J. Clim.*, *14*, 2079–2087.

Stigebrandt, A. (1984), The North Pacific: A global-scale estuary, *J. Phys. Oceanogr.*, *14*, 464–470.

Taylor, J. R., K. K. Falkner, U. Schauer, and M. P. Meredith (2003), Quantitative considerations of dissolved barium as a tracer in the Arctic Ocean, *J. Geophys. Res.*, *108*(C12), 3374, doi:10.1029/2002JC001635.

Vinje, T. (2001), Fram Strait ice fluxes and atmospheric circulation: 1950–2000, *J. Clim.*, *14*, 3508–3517.

Vinje, T., N. Nordlund, and A. Kvarnbekk (1998), Monitoring ice thickness in Fram Strait, *J. Geophys. Res.*, *103*, 10,437–10,449.

Walsh, J. E., X. Zhou, A. Portis, and M. C. Serreze (1994), Atmospheric contribution to hydrologic variations in the Arctic, *Atmos. Ocean*, *32*, 733–755.

Wehl, P. K. (1968), The role of the oceans in climate change: A theory of the ice ages, *Meteorol. Monogr.*, *8*, 38–62.

Widell, K., S. Osterhus, and T. Gammelsrod (2003), Sea ice velocity in the Fram Strait monitored by moored instruments, *Geophys. Res. Lett.*, *30*(19), 1982, doi:10.1029/2003GL018119.

Woodgate, R. A., and K. Aagaard (2005), Revising the Bering Strait freshwater flux into the Arctic Ocean, *Geophys. Res. Lett.*, *32*, L02602, doi:10.1029/2004GL021747.

Woodgate, R. A., K. Aagaard, R. D. Muench, J. Gunn, G. Bjork, B. Rudels, A. T. Roach, and U. Schauer (2001), The Arctic Ocean boundary current along the Eurasian slope and the adjacent Lomonosov Ridge: Water mass properties, transports and transformations from moored instruments, *Deep Sea Res., Part I*, *48*, 1757–1792.

Woodgate, R. A., K. Aagaard, and T. Weingartner (2005a), Monthly temperature, salinity, and transport variability of the Bering Strait throughflow, *Geophys. Res. Lett.*, *32*, L04601, doi:10.1029/2004GL021880.

Woodgate, R. A., K. Aagaard, and T. Weingartner (2005b), A year in the physical oceanography of the Chukchi Sea: Moored measurements from autumn 1990–1991, *Deep Sea Res., Part II*, *52*, 3116–3149.

Zhang, X., and J. Zhang (2001), Heat and freshwater budgets and pathways in the Arctic Mediterranean in a coupled ocean/sea ice model, *J. Oceanogr.*, *57*, 207–234.

_____

K. Aagaard, R. Moritz, M. Steele, and R. A. Woodgate, Polar Science Center, Applied Physics Laboratory, University of Washington, Seattle, WA 98105-6698, USA.

A. P. Barrett, M. C. Serreze, and A. G. Slater, Cooperative Institute for Research in Environmental Sciences, University of Colorado, 1540 30th Street, Boulder, CO 80309, USA. (serreze@kryos.colorado.edu)

R. B. Lammers, Water Systems Analysis Group, University of New Hampshire, Durham, NH 03824, USA.

C. M. Lee, Applied Physics Laboratory, University of Washington, Seattle, WA 98105-6698, USA.

M. Meredith, British Antarctic Survey, Madingley Road, Cambridge CB3 0ET, UK.